Bioorganic & Medicinal Chemistry 19 (2011) 3039–3053

Contents lists available at ScienceDirect

Bioorganic & Medicinal Chemistry

journal homepage: www.elsevier.com/locate/bmc

Design of small molecule inhibitors of acetyl-CoA carboxylase 1 and 2 showing reduction of hepatic malonyl-CoA levels in vivo in obese Zucker rats

Christoffer Bengtsson, Stefan Blaho, David Blomberg Saitton, Kay Brickmann, Johan Broddefalk, Öjvind Davidsson, Tomas Drmota, Rutger Folmer, Kenth Hallberg, Stefan Hallén, Ragnar Hovland, Emre Isin, Petra Johannesson, Bengt Kull, Lars-Olof Larsson, Lars Löfgren, Kristina E. Nilsson, Tobias Noeske, Nick Oakes, Alleyn T. Plowright *, Volker Schnecke, Pernilla Ståhlberg, Pernilla Sörme, Hong Wan, Eric Wellner, Linda Öster

AstraZeneca Research and Development, Pepparedsleden 1, Mölndal 43183, Sweden

ARTICLE INFO

Article history:
Received 3 February 2011
Revised 6 April 2011
Accepted 9 April 2011
Available online 13 April 2011

Keywords:
Acetyl-CoA carboxylase
Malonyl-CoA
Ligand lipophilicity efficiency
Quinoline

ABSTRACT

Inhibition of acetyl-CoA carboxylases has the potential for modulating long chain fatty acid biosynthesis and mitochondrial fatty acid oxidation. Hybridization of weak inhibitors of ACC2 provided a novel, moderately potent but lipophilic series. Optimization led to compounds **33** and **37**, which exhibit potent inhibition of human ACC2, 10-fold selectivity over inhibition of human ACC1, good physical and in vitro ADME properties and good bioavailability. X-ray crystallography has shown this series binding in the CT-domain of ACC2 and revealed two key hydrogen bonding interactions. Both **33** and **37** lower levels of hepatic malonyl-CoA in vivo in obese Zucker rats.

1. Introduction

Obesity and type 2 diabetes mellitus are characterized as worldwide epidemics with associated global deaths of up to 5%.[1] The rate of developing obesity is alarming considering the connection between a body mass index above 30 and diseases such as diabetes, hypertension, artery cardiovascular disease, stroke, and even some forms of cancer. There is a strong demand for drugs capable of treating both obesity and type 2 diabetes mellitus. One biological principle that has been considered for treating these diseases are the enzymes acetyl-CoA carboxylases (ACCs.[a]: EC_6.4.1.2; ACC1 (ACACA); ACC2 (ACACB)).[2] ACCs have pivotal functions in fatty acid metabolism and inhibition of ACCs gives the potential for modulating both long chain fatty acid biosynthesis and mitochondrial fatty acid oxidation. This modulation presents opportunities for treatment of both diabetes and obesity.

ACC is a biotin-dependent protein, composed of a carboxyltransferase (CT), biotin carboxy carrier protein, and biotin carboxylase (BC) domains, which synthesises malonyl-CoA from acetyl-CoA in an ATP-dependent reaction via the fixation of bicarbonate.[3] The synthesis of malonyl-CoA is a two step process where the first reaction occurs in the BC-domain, upon which the biotin is carboxylated. The carboxylated biotin then enters the CT-domain via a narrow channel where carbon dioxide is transferred from the biotin carboxylate to acetyl-CoA to form malonyl-CoA.

Mammalian ACC is known to exist in two isoforms, ACC1 and ACC2. At energy surplus, ACC1 converts acetyl-CoA into malonyl-CoA for de novo lipogenesis in the cytosol while the ACC2 isoform, present on the mitochondrial surface, carries out the same reaction to generate malonyl-CoA for the inhibition of carnitine palmitoyl transferase 1 (CPT-1). The latter reaction constitutes the main regulation of mitochondrial import of fatty acids for β-oxidation. Inhibition of ACCs will cause a switch in cellular substrate handling and favour lipid oxidation, thus preventing deleterious lipids from accumulating in oxidative tissue such as muscle, heart and liver. This reduction in intracellular saturated fatty acids and downstream lipids such as diacylglycerols and ceramide is expected to improve insulin sensitivity. Additionally, the achieved change of lipid flux has the potential to influence whole body energy balance towards an increase of energy expenditure and also correction of dyslipidaemia. In the clinic, failure to maintain weight loss is associated with an impairment of fatty acid oxidation and reduced energy expenditure. These metabolic changes represent a major hurdle in the pharmacotherapy of obesity. Moreover, intramyocellular accumulation of lipids and elevated malonyl-CoA levels are events associated with obesity, leading to reduced oxidative capacity and attenuated insulin sensitivity.[4–6]

* Corresponding author.
E-mail address: alleyn.plowright@astrazeneca.com (A.T. Plowright).

0968-0896/$ - see front matter © 2011 Elsevier Ltd. All rights reserved.
doi:10.1016/j.bmc.2011.04.014

It has been reported that mice with a global deletion in the ACC2 gene have lower body weight, less fat tissue, lower levels of insulin and improved glucose tolerance after long-term exposure to a high fat/high carbohydrate diet, as well as higher rates of fat and carbohydrate oxidation resulting in an increased energy expenditure.[7] Other published data supporting the benefits of ACC suppression derive from a gene silencing approach using specific antisense oligonucleotides to knock-down hepatic ACC1 and/or ACC2. The best result was achieved with a combined ACC1/ACC2 knock-down which caused a significant reduction of hepatic malonyl-CoA levels accompanied by lower liver triglycerides and improved hepatic insulin sensitivity.[8] These results would support the potential for an ACC1/2 isozyme non-selective inhibitor to secure a desirable metabolic profile with increased insulin sensitivity, correction of dyslipidaemia and weight maintenance, as seen in the published knock-out mice. However, there has also been additional research highlighting the complexity and uncertainty regarding the level of selectivity required between the two isoforms. It has been reported that ACC1 knock-out mice show embryonic lethality suggesting that a selective ACC2 inhibitor would be preferred.[9] On the other hand, in 2010 Olson et al. published, contrary to previous results, that mice with either a global deletion of ACC2 or selective deletion of ACC2 from skeletal muscle has no effect on body weight, fat mass, food intake or glucose homeostasis suggesting that selective ACC2 inhibition may be ineffective.[10] Inspired by the potential of the target for treating obesity and type 2 diabetes mellitus a search for potent inhibitors of ACC1 and 2 was initiated. Due to the uncertainty in the literature regarding the impact of inhibiting ACC1 a project was set up to drive on both ACC1 and 2 but ACC2 was the primary data.

The interest in ACC as a target is clearly seen in the increase of number of patent applications and publications in recent years.[2,11] Inhibitors have been reported for both the BC-domain, including the natural product Soraphen,[12], and the CT-domain. Most have focused on the CT-domain (Fig. 1), including the piperidinylpiperidines as exemplified by **1** (CP-640186),[4] the spirochromanone class of compounds such as **2**,[11e] and the (4-piperidinyl)-piperazines such as **3**.[11f] To date, these compounds reported to bind in the CT-domain are isozyme ACC1/2 non-selective inhibitors. Selective inhibitors of ACC2 have been reported with very different chemotypes.[11b,d] However, it has not been reported where these compounds bind.

Herein, we describe the structure–activity relationship and optimization of a series of 1,4-disubstituted cyclohexanes to provide compounds with good potency against the human ACC2 (hACC2) enzyme, moderate 10-fold selectivity against human ACC1 (hACC1) and good physical and ADME properties. To test the concept of ACC inhibition in vivo, we chose to build overall in vivo PK-PD understanding in a stepwise fashion, first establishing target engagement in an acute experiment (lowering of malonyl-CoA in obese Zucker rats) and then examining repeat dosing effects in a disease model. To achieve this, we performed sequentially: 1/intravenous rat PK studies, to obtain in vivo clearance (CL) data; 2/intravenous target engagement studies in obese Zucker rats; 3/oral PK experiments in mice to assess oral absorption/exposure prior to testing in a chronic efficacy study (results not included in the present study). This DMPK data is described for key compounds and the best compounds, **33** and **37**, are shown to provide a good reduction in levels of hepatic malonyl-CoA in vivo in obese Zucker rats.

2. Results and discussion

2.1. Chemistry

The synthesis of the *trans*-1,4-disubstituted cyclohexyl derivatives **17** and **19**–**41** started from commercially available *tert*-butyl {[*trans*-4-(aminomethyl)cyclohexyl]methyl}carbamate **4** (Scheme 1). Coupling of the amine **4** to the carboxylic acids **5** using amide coupling conditions such as EDC/HOBT or TBTU gave the chloro- or bromoamides **6**. Suzuki cross coupling of **6** with the required boronic acid or boronic ester catalysed by either $Pd(PPh_3)_4$ or 1,3-*bis*(2,6-diisopropylphenyl)imidazol-2-ylidene]-(3-chloropyridyl)-palladium(II)dichloride (PEPPSI) gave the derivatives **7**. One derivative, **25**, was alkylated further on the pyrazole with 2-dimethylaminoethylchloride hydrochloride to give **30**. Alternatively, the 2-chloroheteroaromatic derivatives **6** underwent a nucleophilic aromatic substitution reaction with a range of amines to give derivatives **8**. One derivative, **32**, acted as a useful intermediate and could be modified by functional group interconversions to give derivatives **33**, **34** and **37** (Scheme 1). For example, oxidation of **32** under Swern conditions gave an aldehyde that underwent a reductive amination upon treatment with 3-hydroxyazetidine and sodium triacetoxyborohydride to give **37**. Variation of the carbamate was carried out by removing the *tert*-butylcarbamate group in **8** under acidic conditions to provide a primary amine that, upon treatment with either chloroformates or mixed 4-nitrophenylcarbonates,[13] gave the alternative carbamate derivatives **9**.

Alternatively, the required R^3 substituent in **7** or the required amine side chain in **8** was introduced to the carboxylic acid coupling partner prior to reaction with the amine **4**. In some cases the required compounds were commercially available whereas others were synthesised by different methods (Scheme 2). Suzuki cross coupling of the substituted 2-chloro- or 2-bromoheteroaromatic compounds **5** with the required boronic acid or boronic ester catalysed by either $Pd(PPh_3)_4$ or PEPPSI gave the coupling partners **10**. For example, compound **28**, where R^3 = 4-benzylamine was synthesized via this method. Alternatively, **5** could undergo a nucleophilic substitution reaction upon treatment with amines to give **10** where R^3 is an amino substituent. The 2-pyridin-4-ylquinoline-4-carboxylic acid **10** (where R^3 = 4-pyridyl) required to synthesise **24** was prepared by treating 2,3-dihydro-indole-2,3-dione **11** with 4-acetylpyridine and KOH.[14] Finally, 6-phenyl-1*H*-pyrrolo[2,3-*b*]pyridine-4-carboxylic acid required to prepare **21** was synthesised in a

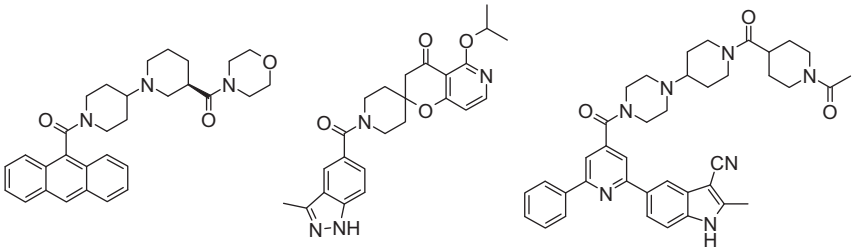

1 (CP-640186)[4] **2** (Pfizer, Compound 59)[11(e)] **3** (Taisho, Compound 13(i))[11(f)]

Figure 1. Structures of ACC inhibitors binding to the CT-domain.

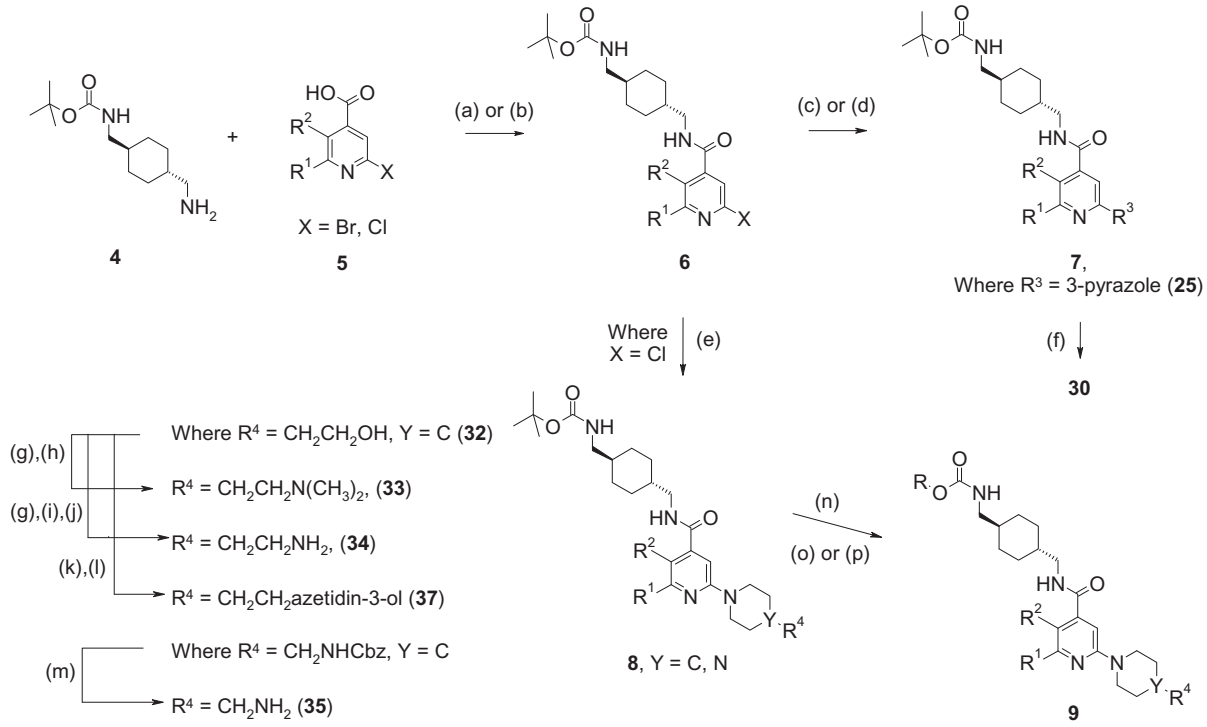

Scheme 1. Reagents and conditions: (a) *N*-methylmorpholine, EDC, HOBT, 2-MeTHF, rt; (b) TBTU, Et_3N, CH_2Cl_2, rt; (c) $R^3B(OH)_2$, $Pd(PPh_3)_4$ K_2CO_3, dioxane, H_2O, 60 °C; (d) $R^3B(OC(CH_3)_2C(CH_3)_2O)$, PEPPSI, K_2CO_3, dioxane, H_2O, 140 °C; (e) RxRyNH, pyridine, 135 °C; (f) Cs_2CO_3, $(CH_3)_2NCH_2CH_2Cl$, EtOH 140 °C; (g) CH_3SO_2Cl, DIPEA, CH_2Cl_2, rt; (h) dimethylamine, DMF, rt; (i) NaN_3, DMF, rt; (j) $SnCl_2$, Et_3N, PhSH, THF, rt; (k) oxalyl chloride, DMSO, Et_3N, CH_2Cl_2, −78 °C to rt; (l) 3-hydroxyazetidine hydrochloride, sodium triacetoxyborohydride, AcOH, EtOH, 120 °C; (m) 5% Pd/C, H_2, rt; (n) (i) HCl, 1,4-dioxane, or (ii) TFA, CH_2Cl_2, rt; (o) EtOC(O)Cl, Et_3N, THF, 0 °C; (p) 4-nitrophenyl tetrahydro-2*H*-pyran-4-yl carbonate (**42**), Et_3N, THF, 40 °C to rt.

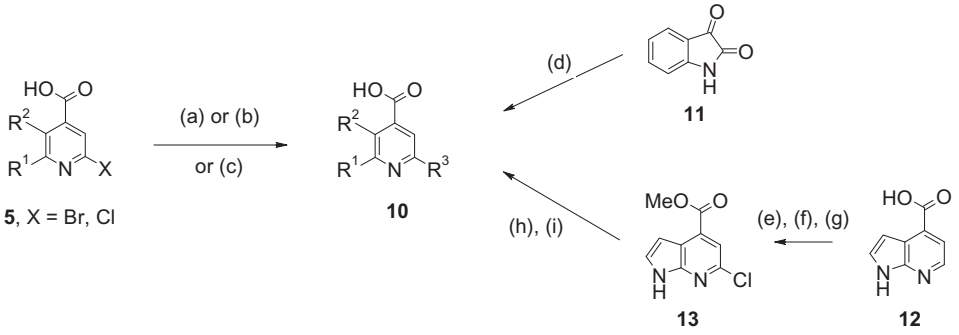

Scheme 2. Reagents and conditions: (a) $R^3B(OH)_2$, $Pd(PPh_3)_4{\cdot}K_2CO_3$, dioxane, H_2O, 60 °C; (b) $R^3B(OC(CH_3)_2C(CH_3)_2O)$, PEPPSI, K_2CO_3, dioxane, H_2O, 140 °C; (c) RxRyNH, pyridine, 135 °C; (d) 4-acetylpyridine, KOH, EtOH, 80 °C; (e) TMS–diazomethane, CH_2Cl_2/MeOH (3:1), rt; (f) *m*-CPBA, DME, rt; (g) ethyl carbonochloridate, HMDS, THF, 50 °C; (h) $R^3B(OH)_2$, *bis*(di-*tert*-butylphosphino)ferrocene palladium dichloride, K_2CO_3, toluene, MeOH, 80 °C; (i) LiOH, 1,4-dioxane, H_2O, 50 °C.

five step sequence starting from 1*H*-pyrrolo[2,3-*b*]pyridine-4-carboxylic acid **12**. Esterification of **12**, followed by oxidation with *meta*-chloroperoxybenzoic acid (*m*-CPBA) and then treatment with ethyl carbonochloridate and hexamethyldisilazane gave methyl 6-chloro-1*H*-pyrrolo[2,3-*b*]-pyridine-4-carboxylate **13**.[15] Cross coupling of **13** with phenylboronic acid using *bis*(di-*tert*-butylphosphino)-ferrocene palladium dichloride as catalyst followed by hydrolysis of the methyl ester with lithium hydroxide gave the required 6-phenyl-1*H*-pyrrolo[2,3-*b*]pyridine-4-carboxylic acid **10** (where R^1 and R^2 make up a pyrrole ring and R^3 = phenyl). Once the required carboxylic acids **10** were in hand they were coupled to the amine **4** under the conditions described in Scheme 1. The *cis*-1,4-disubstituted cyclohexane derivative **18** was synthesized from the same sequence as shown in Scheme 1 but starting from *tert*-butyl {[*cis*-4-(aminomethyl)cyclohexyl]methyl}carbamate, the synthesis of which is described in Supplementary data.[16]

2.2. Discovery of lead compounds

A high throughput screen of the AstraZeneca compound collection provided several hit series feasible for further exploration. Two of the series, represented here by compounds **14** and **15**, were chosen for further work (Fig. 2). Both series had moderate potency versus the hACC2 enzyme and high lipophilicity as measured by logD.[17] Hybridizing compounds **14** and **15** provided either the sulfonamide **16** or the amide **17**. Both compounds showed an improvement in inhibition of hACC2, particularly the amide derivative **17** with a 10-fold improvement in enzyme inhibition.

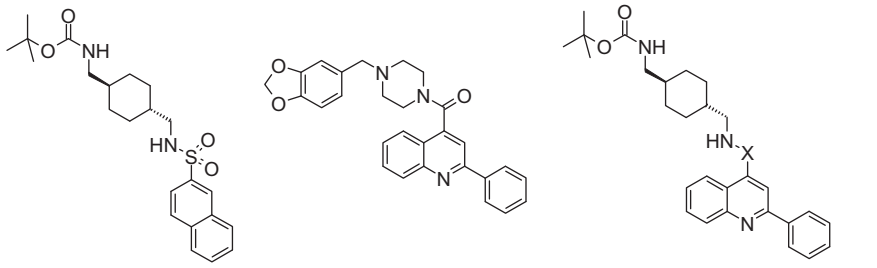

14: hACC2 IC_{50} = 2.5 μM

15: hACC2 IC_{50} = 3.6 μM

16: X = SO_2; hACC2 IC_{50} = 0.69 μM
17: X = CO; hACC2 IC_{50} = 0.21 μM

18: X = CO, *cis*-1,4-cyclohexyl core; hACC2 IC_{50} = 1.0 μM

Figure 2. High throughput screening hits and hybridized *cis*- and *trans*-cyclohexyl derivatives.

However, this compound suffered from high lipophilicity (log *D* = 5.9) leading to poor physical properties such as low solubility (<1 μM) and high human plasma protein binding (fraction unbound = 0.1%). It was considered critical to improve these parameters at this early stage to enable effective testing of compounds throughout the project screening cascade and to achieve the required free compound concentrations to give an opportunity to provide significant in vivo effects. Amide **17** had good permeability as measured in the caco-2 assay (P_{app} A–B 22×10^{-6} cm s^{-1}) but underwent rapid oxidative metabolism leading to high intrinsic CL in vitro in human liver microsomes (HLM, CLint = 124 μL/min/mg).[18] It is known that high plasma protein binding can mask a compound from CL lowering its in vivo CL. However, dosing of **17** intraveneously in rat in vivo DMPK experiments gave rapid CL (60 mL/min/Kg). When the plasma protein binding in rat (fraction unbound = 0.5%) was taken into account the unbound CL (CLu) in vivo was very high (12,000).[19] Hence, the focus was to improve physical properties including solubility and plasma protein binding and reduce both the intrinsic metabolic instability and CLu of the compounds in vivo whilst maintaining or improving potency versus hACC2 to enable effective testing of ACC inhibition in vivo.

The role of lipophilicity has been widely reported in the literature as an important parameter for designing compounds to improve both physical and ADME properties.[20] Clearly it is of paramount importance to also take into account the potency of the compounds and therefore the challenge is to find ligands that are sufficiently potent in the optimal lipophilicity range. As a result the use of the composite parameter ligand lipophilicity efficiency (LLE), calculated as pIC_{50}–log *D* was used.[21] LLE is a measure of how efficiently a compound uses its lipophilicity to drive potency and is used as a means to assess compound efficiency and help analyse SAR within a series. Given the high lipophilicity of this series and the associated issues the project strategy was to focus on reducing lipophilicity whilst maintaining or improving potency versus hACC2 and therefore LLE was used to assess progress within the series. Given the improved potency and lower lipophilicity of **17** (LLE = 0.8) compared to **16** (LLE = −0.5), chemistry was focused on the amide sub-series. The preferred configuration of the 1,4-disubstituted cyclohexyl ring was also tested. Compound **17** was in the *trans*-configuration, whereas the cyclohexyl derivative in the *cis*-configuration, **18**, showed a fivefold drop in potency versus the hACC2 enzyme (Fig. 2). Therefore all further work was focused on the *trans*-1,4-disubstituted cyclohexyl core.

The phenylquinoline of compound **17** contributes significantly to the overall lipophilicity of the compounds. Hence, the initial focus was to vary this part of the molecule to understand its impact on the inhibition of hACC2. Some of the variations attempted are shown in Table 1. Replacement of the quinoline with a pyridine ring as in **19** led to a large drop in potency versus hACC2. Adding an additional methyl group to the pyridyl ring (**20**) failed to bring back any potency and converting the pyridine in **20** to a 1,3-pyrimidine resulted in significantly weaker inhibition of hACC2 (data not

Table 1
Quinoline replacements and substitutions

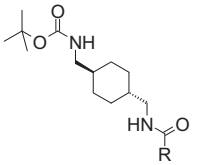

Compd	R	hACC2[a] (μM)	hACC1[a] (μM)	Log *D*	LLE
19	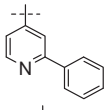	4.5	6.6	4.7	0.6
20	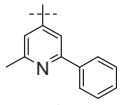	5.8	8.3	5.3	0
21	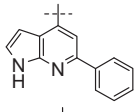	0.78	ND	4.7	1.5
22	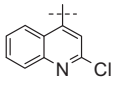	3.8	10	4.9	0.5
23	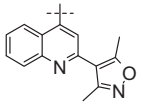	2.9	ND	5.0	0.5
24	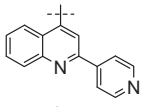	0.21	1.1	4.4	2.3
25	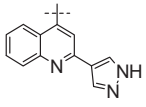	0.57	2.3	3.5	2.7
26	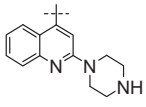	1.3	13	2.9	3.0

[a] The IC_{50} values are reported as means of at least two separate determinations with a typical standard deviation of less than ±30%. ND means not determined.

shown). Attempts to replace the quinoline ring with alternative, less lipophilic bicyclic heterocyclic systems such as pyrrolopyridine **21** also led to a reduction of inhibition of hACC2. With no success in removing or replacing the quinoline ring system the strategy turned to replacing the phenyl ring attached in the 2-position. Initial attempts to replace the phenyl ring with smaller, less lipophilic substituents such as chloro (**22**) or methoxymethyl (data not shown) also led to a significant drop in potency. An alternative way to reduce the overall lipophilicity was to replace the phenyl ring with less lipophilic heterocycles. However, many of the heterocyclic phenyl replacements tested gave a significant reduction in potency (e.g., isoxazole **23**). Only two replacements were more interesting; the pyridyl derivative **24** was equipotent with **17** and the pyrazole derivative **25** gave a ~3-fold reduction in potency compared to **17**. Whilst potency was not improved, both **24** and **25** were much less lipophilic compared to **17**. Hence, despite the knowledge that the potency would need to be improved, the LLE of these derivatives was improved. Finally, replacing the phenyl ring with piperazine to give **26**, also gave a reduction in potency but also a significant reduction in log *D* leading to an improvement in LLE. Despite the reduction in lipophilicity of many of these compounds they still had poor physical properties and low metabolic stability. For example, the pyridyl derivative **24** had low solubility (<1 μM) and low stability in HLM (CLint = 146 μL/min/mg).

All attempts to replace the phenylquinoline moiety, with the exception of **24**, resulted in a loss of potency. Despite an increase in LLE for some derivatives, a boost in potency and a significant improvement in both physicochemical and CL properties was required. Additional studies, including NMR studies of ACC2 in a competitive binding study, revealed that these compounds bind reversibly to the CT-domain in the same site reported in the published X-ray structures of **1** (data not shown).[22,23] It was hypothesized that the phenylquinoline moiety of **17** occupied the same area of space as the anthracene ring system in **1**. Further analysis of the X-ray structure of **1** revealed that the anthracene group is oriented close to the hydrophilic surface of the protein. This presented an opportunity to substitute the phenyl ring of **17** with small polar substituents in an attempt to pick up interactions with the more hydrophilic exterior of the protein to increase potency whilst simultaneously reducing the lipophilicity of the compounds to improve the overall properties. Introduction of a small, basic side chain by replacing the phenyl ring with a benzylamine group showed positive results, especially with the 3-substituted derivative **27** giving a good improvement in potency (Table 2). Compound **27** showed a major improvement in stability in HLM (Table 3). However, the unbound clearance in vivo was still very high. Also, despite the significant decrease in log *D*, the physicochemical properties of **27** remained poor. Compound **27** also showed significant inhibition of the cytochrome P450 isoforms 2C9, 3A4 and 1A2 (IC_{50} values of 0.8, 2.4 and 4 μM, respectively). Attempts were also made to introduce acidic side chains such as in **29**. However, this led to a reduction in potency versus hACC2.

As mentioned, replacement of the phenyl ring in **17** with a pyrazole or piperazine led to a decrease in potency but an improvement in the LLE due to the significant reduction in log *D* compared with the starting phenyl derivative **17**. Based on the increase in potency achieved with **27** it was hypothesized that introducing small basic side chains to both the pyrazole **25** and the piperazine derivative **26** could improve the inhibition of hACC2. Hence, the pyrazole and piperazine derivatives, **30** and **31**, were prepared but only gave a ~2-fold improvement in potency against hACC2 compared with the unsubstituted compounds **25** and **26**, respectively (Table 2). However, the properties of **31** were considerably improved compared with both **17** and **27** (good solubility (73 μM), excellent stability in HLM (<12 μL/min/mg) and no activity against a panel of cytochrome P450 isoforms (1A2, 2C9, 2C19, 2D6, 3A4; <50% inhibition at 13 μM)). Replacement of the piperazine ring in **31** with a piperidine led to **33**, which gave an improvement in potency whilst maintaining the log *D*. Furthermore, **33** again displayed high solubility, good stability in HLM and also high permeability in the caco-2 assay (Table 3). Compound **33** also had significantly reduced human plasma protein binding and a much reduced CLu in vivo in rat so overall a significant improvement compared with both **17** and **27**. Attempts were made to reduce the molecular weight by preparing the primary amine derivative **34** and this compound again displayed good inhibition of hACC2 (IC_{50} = 0.089 μM). However, the introduction of two additional hydrogen bond donors significantly reduced the permeability

Table 2
Substitution of phenyl and heterocyclic ring side chains

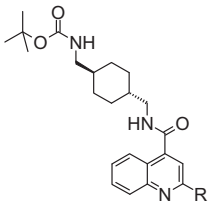

Compd	R	hACC2[a] (μM)	hACC1[a] (μM)	Log *D*	LLE
27	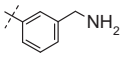	0.052	0.24	3.4	3.9
28	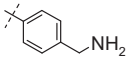	0.33	1.7	3.2	3.3
29	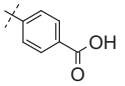	0.75	2.9	2.5	3.6
30	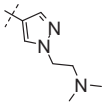	0.24	1.3	3.6	3.0
31	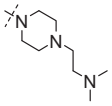	0.73	5.3	3.4	2.8
32	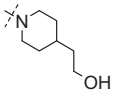	0.23	2.3	4.5	2.1
33	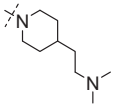	0.11	1.2	3.6	3.3
34	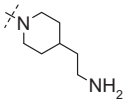	0.089	0.78	3.2	3.8
35		0.69	4.3	3.2	3.0
36	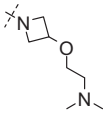	0.63	4.5	3.0	3.2
37	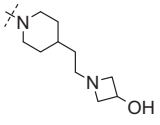	0.099	1.0	3.6	3.5

[a] The IC_{50} values are reported as means of at least two separate determinations with a typical standard deviation of less than ±30%. ND means not determined.

Table 3
Physical property, in vitro ADME and in vivo rat clearance data for **17**, **27**, **33** and **37**

Compd	Solubility[a] (μM)	Fraction unbound[a] (Hu, (%))	HLM[a] (μL/min/mg)	Caco-2 P_{app} A–B[a] (cm s^{-1})	Rat CL[b] (mL/min/Kg)	Rat CLu[c]
17	<1	0.1	124	22	60	12,000
27	8	1.4	14	13	104	6120
33	79	3.4	14	9.4	32	800
37	80	3.3	16	1.4	70	2120

[a] See Supplementary data for assay details.
[b] Compounds dosed intravenously at 3–5 μmol/Kg to Sprague–Dawley rats.
[c] Rat unbound clearance defined as rat CL in vivo/fraction unbound (rat).[19]

compared to **33** (P_{app} A–B 0.5 × 10^{-6} cm s^{-1}).[24] Attempts to reduce the length of the side chain, for example, **35**, or vary the heterocyclic ring system further, as in **36**, also reduced the inhibition of hACC2. As the permeability of **33** was good, the side chain was lengthened to try and achieve a further increase in potency. This is exemplified with **37**, which maintained potency and had similar physical and in vitro ADME properties to **33** (Table 3). However, **37** had a different in vivo rat DMPK profile compared to **33** with higher CL and therefore higher CLu and also a higher volume of distribution. Further attempts to modify the properties of the side chain (pK_a, size, substitution) led to no further improvement in potency or ADME properties. Introducing a non-basic side chain such as the hydroxyethyl derivative **32** also gave no further enhancement in the inhibition of hACC2.

In order to use protein structure information in our design efforts, we embarked on the crystal structure elucidation of the CT-domain of hACC2. However, despite extensive efforts, we were not able to grow protein crystals for hACC2 suitable for structure determination. As a backup strategy alternative mammalian analogs were tested and we found that bovine ACC2 (bACC2) crystallized well. Subsequently a crystal structure was obtained for the CT-domain of bACC2 in complex with the benzylamine derivative **28** (Fig. 3) (X-ray coordinates deposited in the Protein Data Bank with accession number 2X24). The CT-domain of bovine and human ACC2 have 83% sequence identity and only one amino acid differs within a 6 Å distance from any atom of **28**.[25] The X-ray structure revealed useful information such as protein–ligand interactions and ligand orientation that can be used to generate ideas how to influence inhibition of hACC2. The X-ray structure and, in particular, the orientation of the bound ligand shows large similarities with previously published structures of yeast and hACC in complex with **1** as shown in Figure 4.[22,23] Compound **28** showed the same two pivotal anchoring points: 1. Gly461 making a hydrogen bonding interaction to the carbonyl oxygen atom of the *tert*-butylcarbamate group and 2. Glu529 establishing a hydrogen bond with the carbonyl oxygen atom of the amide bond linking the quinoline ring to the cyclohexyl core. Additional hACC2 data on derivatives within this series suggests the distance between these two carbonyl oxygen atoms, both functioning as hydrogen bond acceptors, is important for inhibition of the enzyme (data not shown). The binding site in the structure is located at the interface of the two monomers making up the CT-domain (Fig. 5) and, as hypothesized earlier, the X-ray structure shows the basic benzylamine side chain pointing towards the hydrophilic exterior of the protein.

Another important observation from the X-ray structure is the out-of-plane twist of the quinoline system resulting in a 77° dihedral angle between the quinoline ring and the amide group. Noteworthy, there is no favorable π–π interaction of the quinoline system in the binding site contributing to potency. Therefore this does not explain the loss of potency upon replacement of the quinoline ring with pyridine when comparing **17** and **19**. However, a torsional scan analysis provides a rationale for the observed potency drop-off (Fig. 6).[26] A high energy barrier was observed for the amide group being in the plane of the quinoline ring whereas the out-of-plane orientation is energetically favored. The opposite applies to the pyridine ring. In this case an energy of ~2.5 kcal/mol

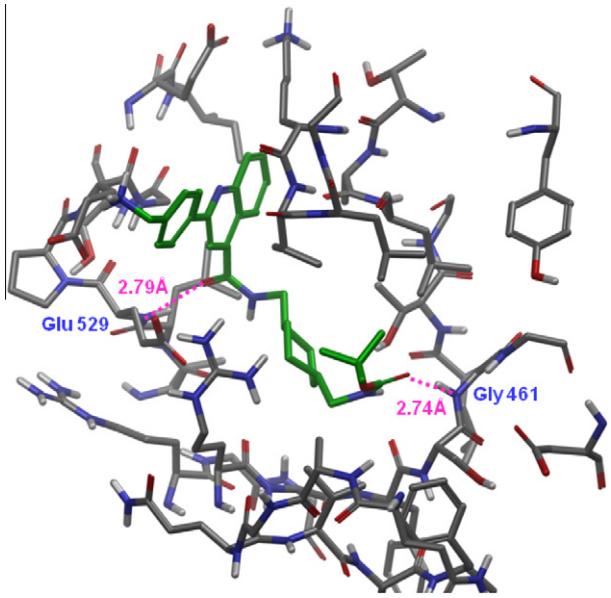

Figure 3. X-ray structure of the CT-domain of bACC2 in complex with the benzylamine derivative **28** (shown in green), highlighting the hydrogen bond coordination between the carbonyl oxygens in **28** and the amino acid residues Glu529 and Gly461.

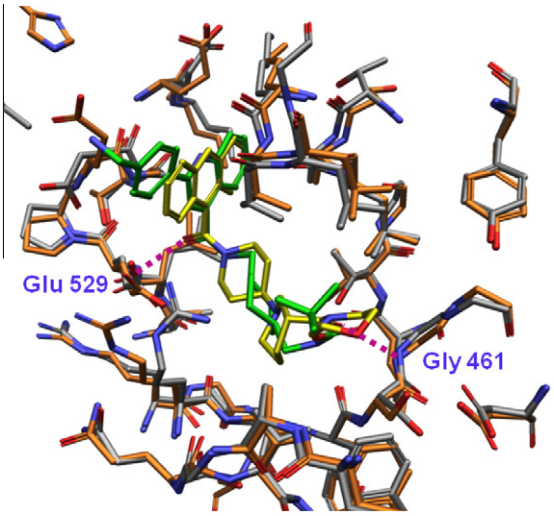

Figure 4. Overlay of the CT-domain of bACC2 (grey) and hACC2 (orange) with the corresponding ligands: **28** (green) and **1** (yellow), respectively. Dashed lines denote the hydrogen bond coordination between the carbonyl oxygens in **1** and the amino acid residues Glu529 and Gly461 in hACC2.

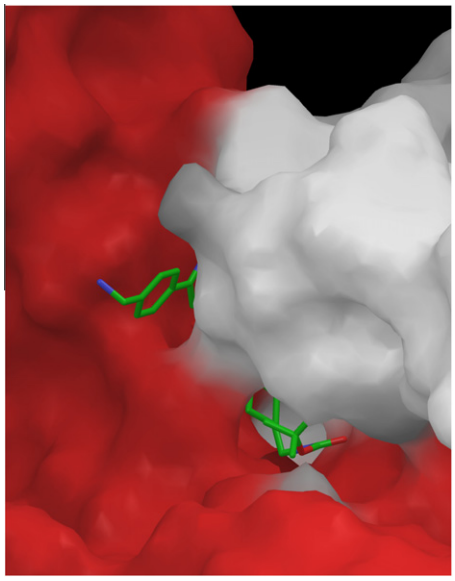

Figure 5. The surface of bACC2 showing the structure of **28** (in green) binding at the interface of the two chains making up the CT-domain. The red and grey colours of the surface show the separate monomers with the benzylamine side chain of **28** pointing out of the exterior of the protein (the blue atom is the amine functionality of **28**).

is required to force the amide group out of the pyridine plane into the ~77° angle it adopts when bound to the protein (red line), which, in turn, negatively affects the binding energy of the whole molecule. Hence the quinoline displays greater potency versus hACC2.

The *tert*-butylcarbamate group contributes a large degree to the overall lipophilicity of the compounds. The potential chemical instability of a *tert*-butylcarbamate group at low pH is also well known as it is commonly used as a protective group for amines. Hence, alternative carbamate replacements for the *tert*-butylcarbamate group were sought. Chemistry was carried out rapidly as described in Scheme 1 to synthesize a broad range of carbamate derivatives, four of which are shown in Table 4. Replacing the *tert*-butylcarbamate with an ethyl carbamate (**38**) to lower both molecular weight and lipophilicity gave a 10-fold drop in potency.

Table 4
tert-Butyl carbamate replacements

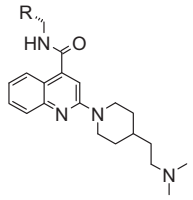

Compd	R	hACC2[a] (μM)	hACC1[a] (μM)	Log *D*	LLE
38	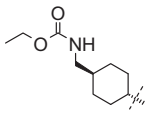	1.4	8.0	2.6	3.3
39	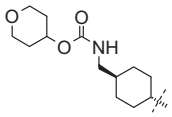	0.68	6.3	2.3	3.9
40	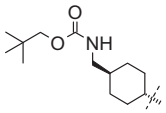	0.13	1.0	4	2.9
41	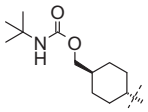	1.7	9.9	3.6	2.2

[a] The IC_{50} values are reported as means of at least two separate determinations with a typical standard deviation of less than ±30%. ND means not determined.

Introduction of the tetrahydropyranylcarbamate (**39**) to reduce lipophilicity gave a fivefold drop in potency versus hACC2. Overall LLE was improved but this did not provide the required level of potency to allow further progress of these compounds. Increasing the size of the *tert*-butyl group to give the *neo*-pentyl derivative **40** to reduce the risk of acid instability showed similar potency versus hACC2 compared to **33**. Finally, reversing the carbamate as in **41** led to a significant reduction of inhibition of hACC2.[16] In summary, all attempts to replace to *tert*-butyl group, with the exception of the *neo*-pentyl lipophilic substituent, led to a drop in potency indicating the need for a lipophilic group in this part of the molecule.

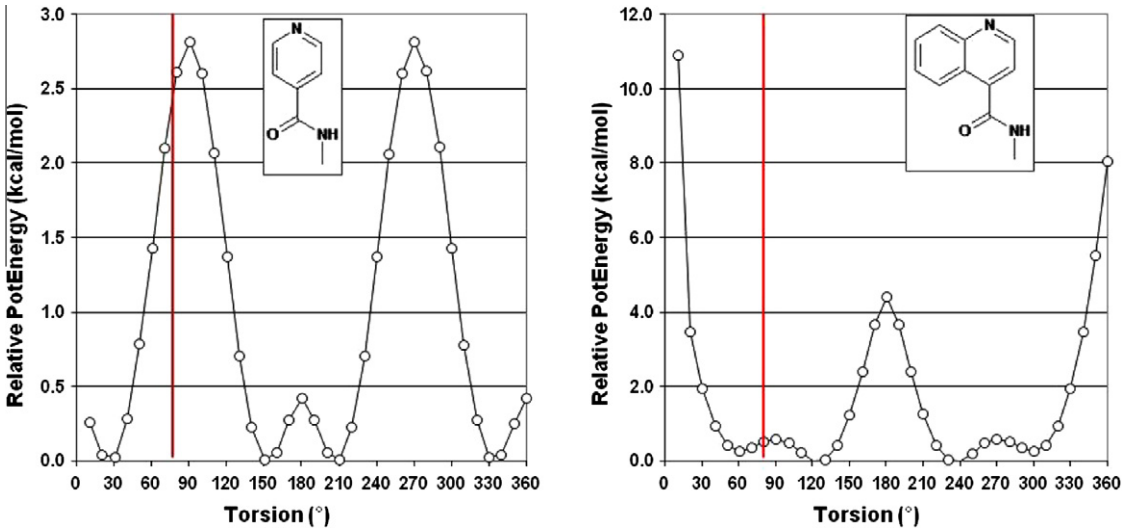

Figure 6. Torsional scan analysis of the amide bond relative to the ring system in 10° increments, starting from the depicted orientation. The red vertical line at 77° denotes the dihedral angle of the carbonyl-quinoline system in the X-ray crystal structure of **28**.

Table 5
Pharmacokinetic data for **33**, **37** and **40** in mice[a]

Compd	CL (mL/min/Kg)	Volume of distribution (L/Kg)	Oral half life, $t_{1/2}$ (h)	Oral bioavailability (%)
33	46	6.7	4.5	131
37	33	3.6	4.3	135
40	52	9.6	2.9	115

[a] Compounds **33**, **37** and **40** dosed at 20, 5 and 33 μmol/Kg (iv) and 20, 10 and 33 μmol/Kg (po), respectively, to C57BL/6 mice.

This may be rationalized from the X-ray structure, which shows the *tert*-butylcarbamate occupying a lipophilic part of the binding pocket formed by amino acids with lipophilic side chains such as Val267, Leu268, Ala424 and Val427.

Throughout this work, inhibition of hACC2 has been used as the primary driver whilst inhibition of hACC1 was monitored. All compounds tested showed greater inhibition of hACC2 than hACC1 and limited selectivity over hACC1 was observed (Tables 1, 2 and 4). In general, most compounds showed less than five-fold selectivity between IC_{50} values for hACC2 and hACC1. For example, the most potent compound versus hACC2, **27**, also had good potency against hACC1 (Table 2). This is perhaps not surprising when looking at the amino acid sequence identity between hACC1 and 2. The two enzymes show 74% identity when comparing the whole enzyme sequence which is in good agreement with earlier findings.[27] In the CT-domain, where these derivatives bind, there is only one residue that differs between the two hACC isoforms that lies less than 6 Å away from the bound ligand **28**; hACC2 has a serine residue at position 262 compared with a glycine residue in hACC1.[25] The highest selectivity that has been observed over hACC1 was ~10-fold. Interestingly this selectivity is fairly general for compounds where a piperidine ring is joined directly in the 2-position of the quinoline ring. Examples include **32**, **33** and **37** which all display modest 10-fold selectivity versus hACC1.

2.3. In vivo evaluation

Compounds **33**, **37** and **40** displayed good potency versus hACC2 and good physical properties, in vitro ADME and in vivo CL profiles to continue progression. To ensure that the measured caco-2 permeability would translate to good oral absorption in mice to support further testing these compounds were progressed into mouse in vivo DMPK studies and the data is shown in Table 5. All three compounds show medium CL, high volumes of distribution, good half life's after oral dosing and excellent oral bioavailability. The fact that the compounds have a bioavailability of greater than 100% could be due to a number of reasons, including enterohepatic recirculation or extrapolation of the concentration-time curve out to infinity. Instead we used the plasma concentration-time curve to support the progression of the compounds into further studies. Additionally all three compounds showed low inhibition of the hERG encoded potassium channel[28] (**33** and **37**; IC_{50} >33 μM and **40**; IC_{50} 14 μM) and **33** showed no activity against a panel of cytochrome P450 isoforms (1A2, 2C9, 2C19, 2D6, 3A4; <50% inhibition at 13 μM).

The ability of compounds to inhibit ACCs in vivo was tested by examining the lowering of malonyl-CoA in obese Zucker rats. This animal model was selected as it shares many key metabolic disorders with the intended target patient group, obese insulin resistant humans and it has substantially elevated hepatic malonyl-CoA levels compared to lean Zucker rat controls offering a larger treatment window model for detection of inhibition of ACCs. There is a sequence homology between hACC2 and rat ACC2 of 87% for the whole enzyme sequence but to ensure that these compounds were active in the rat they were tested in an in vitro rat ACC2 and ACC1 assay.[29] Compounds **33**, **37** and **1** showed good levels of inhibition of rat ACC2 (IC_{50} values of 0.19, 0.15 and 0.17 μM, respectively) with similar potencies for inhibition of rat ACC2 and ACC1 (rat ACC1 IC_{50} values of 0.46, 0.25 and 0.23 μM, respectively). Compounds **33**, **37** and **1** were administered as a constant intravenous infusion for 2 h. At the end of this period, compound infusion was stopped and hepatic malonyl-CoA levels and compound plasma levels were measured. Key results for these studies are shown in Figure 7 where hepatic malonyl-CoA level is plotted as a function of unbound compound plasma levels normalized to in vitro potency for rat ACC2 inhibition. As can be seen, untreated obese Zucker rats (obese vehicle) exhibited a substantial elevation in levels of malonyl-CoA (~10 nmol/g) compared to the metabolically healthy lean Zucker controls (lean vehicle) (~1 nmol/g). The three compounds successfully reduced hepatic malonyl-CoA levels in an exposure dependent fashion. All three compounds show ~50% reduction in hepatic malonyl-CoA levels with unbound plasma concentrations 2–3-fold above the in vitro IC_{50} for rat ACC2 inhibition. Complete normalization of malonyl-CoA to levels seen in the healthy animals can be achieved at unbound plasma levels between approximately 10-fold and 100-fold the in vitro IC_{50} for rat ACC2 inhibition as shown with higher concentrations of **1**. These data confirm the efficacy of these substances for ACC inhibition in vivo. Note that in Figure 7 substance exposure has been normalized to the IC_{50} for rat ACC2. Since the potencies for inhibition of rat ACC2 and ACC1 are similar for this chemical series the data could equally well be normalized to the corresponding value for rat ACC1. The lack of selectivity in the rat, as well as the relatively high abundance of the two ACC isoforms in the liver means that we are not able to assign relative contributions of the individual isoforms to the observed hepatic malonyl-CoA lowering.

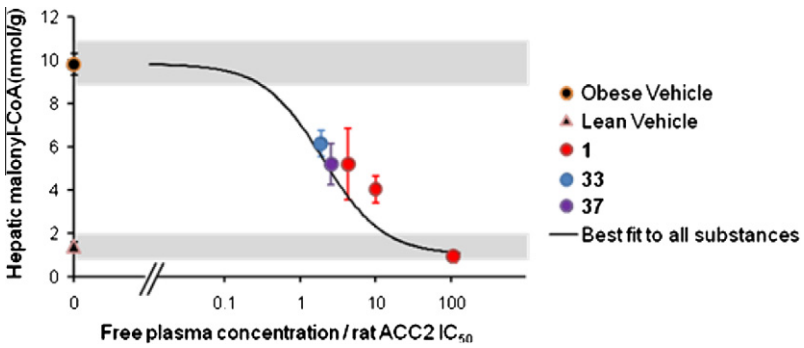

Figure 7. Relationship between hepatic malonyl-CoA levels and unbound compound plasma levels normalized to in vitro potency for rat ACC2 inhibition for **33**, **37** and **1**.

3. Conclusion

A novel series of inhibitors of hACC1 and 2 is described. Hybridising two hit compounds identified from a high throughput screen with IC_{50} values of 2–4 μM versus hACC2 led to a lead series with improved potency but high lipophilicity contributing to poor physical properties, low metabolic stability in vitro and high CLu in vivo. Subsequent optimization led to further improvements in potency, a good reduction in lipophilicity as measured by log *D* and hence a good increase in LLE and resulting improvements in physical properties, stability in HLM and CLu in vivo. Principal to this was the replacement of the phenyl substituent on the quinoline ring with substituted piperidines. X-ray crystallography studies revealed these compounds binding in the CT-domain of the homologous bACC2. The crystal structure of **28** revealed the orientation of the compounds with the small basic side chain extending to the hydrophilic exterior of the enzyme and two key hydrogen bonding interactions that appear crucial in this series of ACC2 inhibitors. Ultimately this work led to **33** and **37**, which exhibit a good balance of properties including potent inhibition of hACC2 in vitro, 10-fold selectivity over inhibition of hACC1, good physical and in vitro ADME properties, significantly improved CLu in rat and good bioavailability in mouse. Both compounds have been shown to lower levels of hepatic malonyl-CoA in vivo in obese Zucker rats. With in vivo target engagement now verified, additional work is required to develop the series further to enhance potency and further improve the DMPK profile. Importantly these compounds, as well as those already reported in the literature, can now be used to further test the concept of ACC2 and ACC1 inhibition including the effects of chronic inhibition and the extent of selectivity required for successful therapeutic intervention.

4. Experimental section

4.1. Synthetic methods

All solvents and reagents were obtained from commercially available sources and used without further purification. Reactions were carried out under nitrogen atmosphere unless otherwise stated. Reactions carried out using a microwave reactor were performed using a Biotage Initiator or Personal Chemistry [Biotage] Emrys Optimizer. Flash chromatography was carried out on prepacked silica gel columns supplied by Biotage and using Horizon/Biotage systems. Analytical HPLC/MS was conducted on a Waters Zevo QTof or Waters LCT Premiere mass spectrometer using an Acquity PDA (Waters) UV detector monitoring either at (a) 210 nm with an Acquity BEH C18 column (2.1 × 100 mm, 1.7 μm, 0.7 mL/min flow rate), using a gradient of 2% v/v CH_3CN in H_2O (ammonium carbonate buffer pH 10) to 98% v/v CH_3CN in H_2O or (b) 230 nm with an Acquity HSS C18 column (2.1 × 100 mm, 1.8 μm, 0.7 mL/min flow rate), using a gradient of 2% v/v CH_3CN in H_2O (ammonium formate buffer pH 3) to 98% v/v CH_3CN in H_2O. Preparative HPLC was conducted using a Waters Fraction Lynx Purification System using either (i) Xbridge Prep C18 5 μm OBD 19 × 150 mm columns, or (ii) Kromasil, C8, 10 μm, 50.8 × 300 mm columns, or (iii) Kromasil, C8, 10 μm, 20 × 50 mm columns. MS-triggered fraction collection was used. All compounds were determined to be >95% pure using the analytical methods (a) or (b) above based on the peak area percentage. ^{1}H NMR spectra were generated on a Varian 300 MHz, Varian 400 MHz, Varian 500 MHz or Varian 600 MHz instrument as indicated. Chemical shifts (δ) are given in parts per million (ppm), with the residual solvent signal used as a reference. Coupling constants (*J*) are reported as Hertz. NMR abbreviations are used as follows: s = singlet, d = doublet, t = triplet, q = quartet, m = multiplet. DMSO/DMSO-d_6* as NMR solvent denotes: wet ^{1}H NMR in DMSO/DMSO-d_6: The solutions are taken from a concentrated sample dissolved in $(CH_3)_2SO$ and are diluted with $(CD_3)_2SO$. Since a substantial amount of $(CH_3)_2SO$ is present in the sample, first a pre-scan is run and analysed to automatically suppress the $(CH_3)_2SO$ (2.54 ppm) and H_2O (3.3 ppm) peaks. This means that in this so-called wet 1D experiment the intensity of peaks that reside in these areas around 3.3 and 2.54 ppm are reduced.

4.1.1. *tert*-Butyl {[*trans*-4-({[(2-phenylquinolin-4-yl)carbonyl]-amino}methyl)cyclohexyl]methyl}carbamate (17)

2-Phenyl-quinoline-4-carboxylic acid (200 mg, 0.80 mmol) was dissolved in CH_2Cl_2 (8 mL) and *tert*-butyl {[*trans*-4-(aminomethyl)-cyclohexyl]methyl}carbamate (**4**, 204 mg, 0.84 mmol), TBTU (283 mg, 0.88 mmol) and Et_3N (0.45 mL, 3.2 mmol) were added and the reaction mixture was stirred at rt for 15 h. The reaction mixture was concentrated in vacuo to leave a residue, which was dissolved in DMSO and purified by HPLC, using a gradient of 40–100% mobile phase A (100% CH_3CN) over 30 min (mobile phase B = 5% CH_3CN + 95% 0.1 M NH_4OAc) to give the title compound as a white solid (247 mg, 65%). ^{1}H NMR (400 MHz, DMSO-d_6) δ 8.77 (t, *J* = 5.6 Hz, 1H), 8.29–8.23 (m, 2H), 8.14–8.04 (m, 3H), 7.81–7.75 (m, 1H), 7.64–7.46 (m, 5H), 3.19 (t, *J* = 6.1 Hz, 2H), 2.74 (t, *J* = 6.2 Hz, 2H), 1.80 (d, *J* = 11.1 Hz, 2H), 1.68 (d, *J* = 11.5 Hz, 2H), 1.57–1.45 (m, 1H), 1.33 (s, 9H), 1.32–1.22 (m, 1H), 1.00–0.76 (m, 4H); HRMS (ESI) *m/z* calcd for $C_{29}H_{36}N_3O_3$ $[M+H]^+$ 474.2757; found 474.2773.

4.1.2. *tert*-Butyl {[*cis*-4-({[(2-phenylquinolin-4-yl)carbonyl]-amino}methyl)cyclohexyl]methyl}-carbamate (18)

Prepared as a solid using essentially the same procedure as described for **17** starting from *tert*-butyl {[*cis*-4-(aminomethyl)-cyclohexyl]-methyl}carbamate[16] in place of **4**. ^{1}H NMR (500 MHz, $CDCl_3$) δ 8.15 (d, *J* = 8.3 Hz, 1H), 8.11 (dd, *J* = 8.2, 1.3 Hz, 3H), 7.82 (s, 1H), 7.76–7.70 (m, 1H), 7.55–7.45 (m, 4H), 6.33 (t, *J* = 5.8 Hz, 1H), 4.60 (s, 1H), 3.47 (t, *J* = 6.7 Hz, 2H), 3.07 (t, *J* = 6.4 Hz, 2H), 1.85 (s, 1H), 1.71–1.38 (m, 18H); HRMS (ESI) *m/z* calcd for $C_{29}H_{36}N_3O_3$ $[M+H]^+$ 474.2757; found 474.2764.

4.1.3. *tert*-Butyl [(*trans*-4-{[(2-phenylisonicotinoyl)amino]-methyl}cyclohexyl)methyl]carbamate (19)

2-Bromo-isonico-tinic acid (0.92 g, 4.5 mmol), TBTU (1.6 g, 5.0 mmol) and DIPEA (1.1 g, 8.3 mmol) were added to a solution of **4** (1.0 g, 4.1 mmol) in DMF (10 mL) and the reaction mixture was stirred at rt for 22 h. Water was added to give a precipitate which was filtered to give the intermediate amide (1.7 g, 96%). The amide (62 mg, 0.15 mmol) was dissolved in CH_3CN (3 mL) and treated with phenylboronic acid (32 mg, 0.26 mmol), $Pd(OAc)_2$ (14 mg, 0.06 mmol), and a 1 M aqueous solution of $NaHCO_3$ (1 mL). The reaction mixture was sealed, degassed with nitrogen for 15 min, and heated in a microwave reactor at 150 °C for 10 min. The solvent was concentrated in vacuo to leave a residue. The residue was dissolved in CH_2Cl_2 and washed with a saturated aqueous solution of $NaHCO_3$ and then dried using a phase separator. The solvent was concentrated in vacuo to leave a residue which was purified by flash chromatography, using EtOAc/heptane (2:1) + 1% Et_3N as eluent, to give the title compound as a white solid (33 mg, 53%). ^{1}H NMR (500 MHz, $CDCl_3$) δ 8.80 (d, *J* = 5.0 Hz, 1H), 8.09–8.03 (m, 3H), 7.54–7.43 (m, 4H), 6.43–6.32 (m, 1H), 4.65–4.57 (m, 1H), 3.36 (t, *J* = 6.4 Hz, 2H), 2.99 (t, *J* = 6.2 Hz, 2H), 1.91–1.78 (m, 4H), 1.67–1.55 (m, 2H), 1.45 (s, 9H), 1.10–0.90 (m, 4H); HRMS (ESI) *m/z* calcd for $C_{25}H_{34}N_3O_3$ $[M+H]^+$ 424.2600; found 424.2610.

4.1.4. *tert*-Butyl [(*trans*-4-{[(2-methyl-6-phenylisonicotinoyl)-amino]methyl}cyclohexyl)methyl]carbamate (20)

Prepared as a solid using essentially the same procedure as described for **19** starting from 2-chloro-6-methylisonicotinic acid

in place of 2-bromoisonicotinic acid. ^{1}H NMR (500 MHz, $CDCl_3$) δ 8.03–7.99 (m, 2H), 7.81 (s, 1H), 7.50–7.45 (m, 2H), 7.45–7.40 (m, 1H), 7.36 (s, 1H), 6.25 (s, 1H), 4.58 (s, 1H), 3.34 (t, J = 6.4 Hz, 2H), 2.98 (t, J = 6.2 Hz, 2H), 2.68 (s, 3H), 1.90–1.76 (m, 4H), 1.44 (s, 9H), 1.37–1.23 (m, 2H), 1.10–0.90 (m, 4H); HRMS (ESI) m/z calcd for $C_{26}H_{36}N_3O_3$ $[M+H]^+$ 438.2757; found 438.2751.

4.1.5. *tert*-Butyl ((*trans*-4-((6-phenyl-1*H*-pyrrolo[2,3-*b*]-pyrid-ine-4-carboxamido)methyl)cyclohexyl)methyl-carbamate (21)

Prepared as a solid using essentially the same procedure as described for **17** starting from 6-phenyl-1*H*-pyrrolo[2,3-*b*]pyridine-4-carboxylic acid[16] in place of 2-phenyl-quinoline-4-carboxylic acid. ^{1}H NMR (600 MHz, DMSO/DMSO-d_6*) δ 11.85 (s, 1H), 8.63 (t, J = 5.8 Hz, 1H), 8.16–8.10 (m, 2H), 7.92 (s, 1H), 7.58–7.54 (m, 1H), 7.51–7.46 (m, 2H), 7.42–7.36 (m, 1H), 6.78–6.73 (m, 2H), 3.16 (t, J = 6.3 Hz, 2H), 2.75–2.72 (m, 2H), 1.78 (d, J = 11.1 Hz, 2H), 1.68 (d, J = 12.6 Hz, 2H), 1.56–1.48 (m, 1H), 1.33 (s, 9H), 1.32–1.25 (m, 1H), 0.97–0.73 (m, 4H); HRMS (ESI) m/z calcd for $C_{27}H_{35}N_4O_3$ $[M+H]^+$ 463.2709; found 463.2674.

4.1.6. *tert*-Butyl{[*trans*-4-({[(2-chloroquinolin-4-yl)carbonyl]-amino}methyl)cyclohexyl]methyl}-carbamate (22)

N-Methyl morpholine (5.9 mL, 54 mmol) and **4** (6.7 g, 28 mmol) were added to a solution of 2-chloroquinoline-4-carboxylic acid (5.6 g, 27 mmol) in a mixture of 2-MeTHF (50 mL) and H_2O (34 mL) at rt. An aqueous solution (9 mL) of HOBt (20% w/w) and *N*-methyl morpholine (15% w/w) was added to the stirred solution followed by the addition of EDC (6.7 g, 35 mmol). The reaction mixture was stirred vigorously at rt for 4 days. The mixture was filtered and the collected solid was washed with water containing 10% MeOH to leave the title compound as an off-white solid (6.6 g, 57%): ^{1}H NMR (400 MHz, DMSO-d_6) δ 8.81 (t, J = 5.7 Hz, 1H), 8.07 (d, J = 8.4 Hz, 1H), 7.99 (d, J = 8.4 Hz, 1H), 7.89–7.81 (m, 1H), 7.73–7.66 (m, 1H), 7.59 (s, 1H), 6.77 (t, J = 5.6 Hz, 1H), 3.21–3.12 (m, 2H), 2.79–2.72 (m, 2H), 1.83–1.74 (m, 2H), 1.72–1.64 (m, 2H), 1.56–1.43 (m, 1H), 1.35 (s, 9H), 1.33–1.24 (m, 1H), 0.90–0.75 (m, 4H); HRMS (ESI) m/z calcd for $C_{23}H_{31}ClN_3O_3$ $[M+H]^+$ 432.2054; found 432.2072.

4.1.7. *tert*-Butyl ({*trans*-4-[({[2-(3,5-dimethylisoxazol-4-yl)-quinolin-4-yl]carbonyl}amino)-methyl]cyclohexyl}methyl)-carbamate (23)

2-Chloroquinoline-4-carboxylic acid (0.15 g, 0.72 mmol), 3,5-dimethylisoxazole-4-boronic acid (0.12 g, 0.87 mmol) and $Pd(PPh_3)_4$ (42 mg, 0.04 mmol) were added to a mixture of dioxane (2 mL) and a 1 M aq solution of K_2CO_3 (2 mL). The reaction mixture was degassed, sealed, and heated in a microwave reactor at 140 °C for 15 min. The reaction mixture was concentrated in vacuo to leave a residue which was purified by HPLC using a gradient of 30–100% mobile phase A (100% CH_3CN) over 30 min (mobile phase B = 5% CH_3CN + 95% 0.1 M NH_4OAc) to give the intermediate carboxylic acid (148 mg, 75%). m/z 269.6 $(M+H)^+$. The intermediate carboxylic acid was then coupled to **4** using essentially the same method as for **17** to give the title compound as a solid. ^{1}H NMR (400 MHz, DMSO-d_6) δ 8.76 (t, J = 5.5 Hz, 1H), 8.12–8.04 (m, 2H), 7.83 (t, J = 7.3 Hz, 1H), 7.71–7.60 (m, 2H), 6.79 (s, 1H), 3.22 (t, J = 6.0 Hz, 2H), 2.77 (t, J = 6.1 Hz, 2H), 2.69 (s, 3H), 2.50 (s, 3H), 1.81 (d, J = 10.9 Hz, 2H), 1.72 (d, J = 11.6 Hz, 2H), 1.60–1.47 (m, 1H), 1.37 (s, 9H), 1.35–1.26 (m, 1H), 1.05–0.79 (m, 4H); HRMS (ESI) m/z calcd for $C_{28}H_{37}N_4O_4$ $[M+H]^+$ 493.2815; found 493.2821.

4.1.8. *tert*-Butyl {[*trans*-4-({[(2-pyridin-4-ylquinolin-4-yl)carbonyl]amino}methyl)-cyclohexyl]methyl}-carbamate (24)

Potassium hydroxide (0.57 g, 10 mmol) was added to a mixture of 2,3-dihydro-indole-2,3-dione (isatin) (0.50 g, 3.4 mmol) and 4-acetylpyridine (0.50 g, 4.1 mmol) in EtOH (4 mL) and the reaction mixture was heated at 80 °C for 20 h. The reaction mixture was diluted with water and purified by HPLC using a gradient of 0–100% mobile phase A (100% CH_3CN) over 30 min (mobile phase B = 5% CH_3CN + 95% 0.1 M NH_4OAc) to give the intermediate 2-pyridin-4-ylquinoline-4-carboxylic acid (0.20 g, 17%). The intermediate 2-pyridin-4-ylquinoline-4-carboxylic acid was then coupled to **4** in a similar way to that described for **17** to give the title compound as a solid. ^{1}H NMR (400 MHz, DMSO-d_6) δ 8.83 (t, J = 5.6 Hz, 1H), 8.81–8.77 (m, 2H), 8.29–8.25 (m, 2H), 8.22 (s, 1H), 8.21–8.15 (m, 2H), 7.90–7.84 (m, 1H), 7.75–7.68 (m, 1H), 6.79 (t, J = 5.6 Hz, 1H), 3.24 (t, J = 6.1 Hz, 2H), 2.78 (t, J = 6.2 Hz, 2H), 1.84 (d, J = 11.0 Hz, 2H), 1.73 (d, J = 11.7 Hz, 2H), 1.60–1.49 (m, 1H), 1.37 (s, 9H), 1.34–1.27 (m, 1H), 1.05–0.75 (m, 4H); HRMS (ESI) m/z calcd for $C_{28}H_{35}N_4O_3$ $[M+H]^+$ 475.2709; found 475.2704.

4.1.9. *tert*-Butyl ({*trans*-4-[({[2-(1*H*-pyrazol-4-yl)quinolin-4-yl]-carbonyl}amino)methyl]cyclohexylmethyl)carbamate (25)

4-(4,4,5,5-Tetramethyl-1,3,2-dioxaborolan-2-yl)-1*H*-pyrazole (194 mg, 1.00 mmol) and **22** (290 mg, 0.67 mmol) were dissolved in dioxane (3 mL) and PEPPSI (11 mg, 0.017 mmol) and a solution of K_2CO_3 (176 mg, 1.27 mmol) in water (3 mL) were added. The reaction mixture was heated in a microwave reactor at 140 °C for 30 min and then a saturated aqueous solution of $NaHCO_3$ was added. The layers were separated and the aqueous layer was extracted with EtOAc. The combined organic layers were concentrated in vacuo and purified by flash chromatography using a gradient of 0 to 15% EtOAc in hexane as eluent. Further purification was achieved by dissolving the title compound in DMSO and purifying by HPLC, using varying gradients of CH_3CN and 0.2% NH_3 buffer to give the title compound as a solid (20 mg, 9%). ^{1}H NMR (400 MHz, DMSO-d_6) δ 8.75 (t, J = 5.6 Hz, 1H), 8.58 (s, 1H), 8.25 (s, 1H), 8.02–7.96 (m, 2H), 7.86 (s, 1H), 7.77–7.71 (m, 1H), 7.57–7.51 (m, 1H), 6.79 (t, J = 5.6 Hz, 1H), 6.25 (t, J = 1.9 Hz, 1H), 3.21 (t, J = 6.2 Hz, 2H), 2.78 (t, J = 6.3 Hz, 2H), 1.83 (d, J = 11.0 Hz, 2H), 1.72 (d, J = 11.0 Hz, 2H), 1.59–1.47 (m, 1H), 1.37 (s, 9H), 1.36–1.26 (m, 1H), 1.02–0.80 (m, 4H); HRMS (ESI) m/z calcd for $C_{26}H_{34}N_5O_3$ $[M+H]^+$ 464.2661; found 464.2671.

4.1.10. *tert*-Butyl {[*trans*-4-({[(2-piperazin-1-ylquinolin-4-yl)-carbonyl]amino}methyl)cyclohexyl]methyl}carbamate (26)

Piperazine (239 mg, 2.78 mmol) was added to a solution of **22** (100 mg, 0.23 mmol) in pyridine (2 mL) and the reaction mixture was heated to 130 °C for 30 min in a microwave reactor. The reaction mixture was concentrated in vacuo to leave a residue which was purified by flash chromatography, using a gradient of 5–70% MeOH (2% Et_3N) in CH_2Cl_2 as eluent, and then HPLC, using a gradient of 30–100% CH_3CN and 0.2% NH_3 buffer as eluent to give the title compound as a solid (43 mg, 39%). ^{1}H NMR (300 MHz, $CDCl_3$) δ 8.61–8.56 (m, 1H), 7.80–7.77 (m, 1H), 7.57–7.48 (m, 3H), 7.23–7.18 (m, 1H), 6.79–6.74 (m, 1H), 3.63–3.58 (m, 4H), 3.16–3.10 (m, 2H), 2.81–2.73 (m, 6H), 1.81–1.75 (m, 2H), 1.72–1.66 (m, 2H), 1.52–1.44 (m, 1H), 1.36 (s, 9H), 1.32–1.26 (m, 1H), 0.96–0.80 (m, 4H); HRMS (ESI) m/z calcd for $C_{27}H_{40}N_5O_3$ $[M+H]^+$ 482.3131; found 482.3124.

4.1.11. *tert*-Butyl [(*trans*-4-{[({2-[3-(aminomethyl)phenyl]-quinolin-4-yl}carbonyl)amino]methyl}cyclohexyl)methyl]-carbamate (27)

Prepared using essentially the same procedure as described for **23** starting from **22** (200 mg, 0.49 mmol) and 3-(amino-methyl)-phenyl]boronic acid hydrochloride to give the title compound as a solid (109 mg, 0.58 mmol). ^{1}H NMR (400 MHz, MeOH-d_4) δ 8.21–8.11 (m, 3H), 8.08 (dt, J = 7.4, 1.6 Hz, 1H), 8.02 (s, 1H), 7.84–7.77 (m, 1H), 7.67–7.60 (m, 1H), 7.57–7.48 (m, 2H), 3.96 (s, 2H), 3.35 (d, J = 6.8 Hz, 2H), 2.90 (d, J = 6.7 Hz, 2H), 1.94 (d, J = 12.4 Hz, 2H), 1.83 (d, J = 12.2 Hz, 2H), 1.71–1.58 (m, 1H), 1.43

(s, 10H), 1.15–0.91 (m, 4H); HRMS (ESI) *m/z* calcd for $C_{30}H_{39}N_4O_3$ $[M+H]^+$ 503.3022; found 503.2985.

4.1.12. *tert*-Butyl [(*trans*-4-{[({2-[4-(aminomethyl)phenyl]quinolin-4-yl}carbonyl)amino]methyl}cyclo-hexyl)methyl]carbamate acetate (28)

2-Chloroquinoline-4-carboxylic acid (0.15 g, 0.72 mmol) and 4-(aminomethylphenyl)boronic acid (0.16 g, 0.87 mmol) were reacted under similar conditions to that described for **23**. The reaction mixture was then cooled to 0 °C and a solution of (9-fluorenylmethyl)chloroformate (0.46 g, 1.8 mmol) in dioxane (1 mL) was added dropwise. The reaction mixture was warmed to rt and stirred for 36 h. The reaction mixture was filtered and the solid was washed with DMSO, water and MeOH to give the carboxylic acid (0.22 g, 60% over two steps) as a crude solid, which was used directly in the next step without further purification. The crude acid was reacted with **4** using essentially the same procedure as described for **17** to give the crude amide, which was dissolved in CH_2Cl_2 (4 mL) and treated with piperidine (1 mL). The reaction mixture was stirred at rt for 5 min and then concentrated in vacuo to leave a residue, which was dissolved in DMSO and purified by HPLC, using a gradient of 0–100% mobile phase A (100% CH_3CN) over 30 min (mobile phase B = 5% CH_3CN + 95% 0.1 M NH_4OAc) to give the title compound as a solid (35 mg, 32%). ^{1}H NMR (400 MHz, DMSO-d_6) δ 8.77 (t, J = 5.7 Hz, 1H), 8.21 (d, J = 8.2 Hz, 2H), 8.07 (dd, J = 8.5, 2.7 Hz, 1H), 8.03 (s, 1H), 7.77 (t, J = 7.7 Hz, 1H), 7.61–7.46 (m, 4H), 6.74 (t, J = 5.4 Hz, 1H), 3.77 (s, 2H), 3.19 (t, J = 6.1 Hz, 2H), 2.74 (t, J = 6.2 Hz, 2H), 1.83 (s, 2H), 1.79 (d, J = 12.6 Hz, 2H), 1.68 (d, J = 12.4 Hz, 2H), 1.55–1.45 (m, 1H), 1.33 (s, 9H), 1.30–1.23 (m, 1H), 1.00–0.76 (m, 4H); HRMS (ESI) *m/z* calcd for $C_{30}H_{39}N_4O_3$ $[M+H]^+$ 503.3022; found 503.3018.

4.1.13. 4-(4-{[(*trans*-4-{[(*tert*-Butoxycarbonyl)amino]methyl}-cyclohexyl)methyl]carbamoyl}quinolin-2-yl)benzoic acid (29)

Prepared using essentially the same procedure as described for **28** using (4-methoxycarbonylphenyl)boronic acid in place of 4-(aminomethylphenyl)boronic acid and then similar acid coupling conditions as described for **17** to give the intermediate methyl ester. The methyl ester (13 mg, 0.024 mmol) was dissolved in THF (1 mL) and treated with a 1 M aqueous solution of lithium hydroxide (0.5 mL). The reaction mixture was stirred at rt for 3 h and then concentrated in vacuo to leave a residue. The residue was dissolved in DMSO and purified by HPLC using a gradient of 30–100% mobile phase A (100% CH_3CN) over 30 min (mobile phase B = 5% CH_3CN + 95% 0.1 M NH_4OAc) to give the title compound as a colourless oil (4.7 mg, 39%). ^{1}H NMR (400 MHz, DMSO-d_6) δ 13.05 (s, 1H), 8.87–8.79 (m, 1H), 8.49–8.40 (m, 2H), 8.21–8.09 (m, 5H), 7.85 (t, J = 8.3 Hz, 1H), 7.72–7.65 (m, 1H), 6.80 (t, J = 6.0 Hz, 1H), 3.24 (t, J = 6.2 Hz, 2H), 2.78 (t, J = 6.2 Hz, 2H), 1.88–1.80 (m, 2H), 1.78–1.68 (m, 2H), 1.60–1.49 (m, 1H), 1.37 (s, 9H), 1.36–1.27 (m, 1H), 1.07–0.80 (m, 4H); HRMS (ESI) *m/z* calcd for $C_{30}H_{36}N_3O_5$ $[M+H]^+$ 518.2655; found 518.2651.

4.1.14. *tert*-Butyl {[*trans*-4-({[(2-{1-[2-(dimethylamino)ethyl]-1*H*-pyrazol-4-yl}quinolin-4-yl)carbonyl]-amino}methyl)cyclohexyl]methyl}carbamate (30)

Cesium carbonate (90 mg, 0.28 mmol) and 2-dimethylaminoethylchloride hydrochloride (24 mg, 0.17 mmol) were added to a solution of **25** (64 mg, 0.14 mmol) in EtOH (1 mL) and the reaction mixture was heated in a microwave reactor at 140 °C for 20 min. The reaction mixture was concentrated in vacuo to leave a residue which was purified by HPLC using a gradient of 20–100% mobile phase A (100% CH_3CN) over 25 min (mobile phase B = 5% CH_3CN + 95% 0.1 M HCO_2H) as eluent to give the title compound as a solid (37 mg, 50%). ^{1}H NMR (400 MHz, DMSO-d_6) δ 8.76 (t, J = 5.6 Hz, 1H), 8.55 (s, 1H), 8.20 (s, 1H), 8.03–7.95 (m, J = 11.4, 7.8 Hz, 2H), 7.80 (s, 1H), 7.77–7.71 (m, 1H), 7.58–7.51 (m, 1H), 6.79 (t, J = 5.6 Hz, 1H), 4.27 (t, J = 6.3 Hz, 2H), 3.21 (t, J = 6.2 Hz, 2H), 2.78 (t, J = 6.3 Hz, 2H), 2.71 (t, J = 6.4 Hz, 2H), 2.19 (s, 6H), 1.83 (d, J = 10.8 Hz, 2H), 1.72 (d, J = 10.6 Hz, 2H), 1.58–1.47 (m, 1H), 1.37 (s, 9H), 1.35–1.26 (m, 1H), 1.03–0.80 (m, 4H); HRMS (ESI) *m/z* calcd for $C_{30}H_{43}N_6O_3$ $[M+H]^+$ 535.3397; found 535.3371.

4.1.15. *tert*-Butyl [(*trans*-4-{[({2-[4-(2-hydroxyethyl)piperazin-1-yl]quinolin-4-yl}carbonyl)amino]-methyl}cyclohexyl)methyl]-carbamate (31)

Prepared using essentially the same procedure as **26** using 1-(2-dimethylaminoethyl)-piperazine (0.52 g, 3.3 mmol) in place of piperazine to give the title compound as a solid. ^{1}H NMR (600 MHz, DMSO/DMSO-d_6)* δ 8.58 (t, J = 5.7 Hz, 1H), 7.77 (d, J = 7.4 Hz, 1H), 7.55 (d, J = 7.8 Hz, 1H), 7.53–7.49 (m, 1H), 7.24–7.18 (m, 1H), 7.14 (s, 1H), 6.76 (t, J = 5.9 Hz, 1H), 3.67–3.64 (m, 4H), 3.12 (t, J = 6.2 Hz, 2H), 2.74 (t, J = 6.4 Hz, 2H), 2.43–2.38 (m, 4H), 2.14 (s, 6H), 1.77 (d, J = 12.7 Hz, 2H), 1.68 (d, J = 12.2 Hz, 2H), 1.51–1.43 (m, 1H), 1.34 (s, 9H), 1.30–1.24 (m, 1H), 0.95–0.78 (m, 4H); HRMS (ESI) *m/z* calcd for $C_{31}H_{49}N_6O_3$ $[M+H]^+$ 553.3866; found 553.3854.

4.1.16. *tert*-Butyl [(*trans*-4-{[({2-[4-(2-hydroxyethyl)piperidin-1-yl]quinolin-4-yl}carbonyl)amino]-methyl}cyclohexyl)-methyl]carbamate (32)

Prepared using essentially the same procedure as described for **26** using 4-piperidineethanol in place of piperazine to give the title compound as a solid (50 mg, 51%). ^{1}H NMR (600 MHz, DMSO/DMSO-d_6)* δ 8.57 (t, J = 5.7 Hz, 1H), 7.74 (d, J = 8.2 Hz, 1H), 7.54–7.51 (m, 1H), 7.50–7.46 (m, 1H), 7.19–7.15 (m, 1H), 7.11 (s, 1H), 6.77–6.73 (m, 1H), 4.52–4.46 (m, 2H), 4.43–4.36 (m, 1H), 3.12 (t, J = 6.2 Hz, 2H), 2.90–2.83 (m, 2H), 2.74 (t, J = 6.3 Hz, 2H), 1.79–1.71 (m, 4H), 1.69–1.62 (m, 3H), 1.50–1.42 (m, 1H), 1.38–1.33 (m, 2H), 1.33 (s, 9H), 1.30–1.24 (m, 1H), 1.14–1.05 (m, 2H), 0.94–0.76 (m, 4H); HRMS (ESI) *m/z* calcd for $C_{30}H_{45}N_4O_4$ $[M+H]^+$ 525.3441; found 525.3452.

4.1.17. *tert*-Butyl {[*trans*-4-({[(2-{4-[2-(dimethylamino)ethyl]-piperidin-1-yl}quinolin-4-yl)carbonyl]-amino}methyl)cyclohexyl]-methyl}carbamate (33)

DIPEA (0.3 mL, 1.73 mmol) and methane sulfonyl chloride (158 mg, 1.40 mmol) were added to a solution of **32** (360 mg, 0.69 mmol) in CH_2Cl_2 (10 mL) at 0 °C and the reaction mixture was stirred for 1 h at rt. The reaction mixture was concentrated in vacuo to leave the crude mesylate which was used in the next step with no further purification. Dimethylamine (2 M in MeOH, 1.66 mL, 3.3 mmol) was added to the mesylate (600 mg, 0.17 mmol) in DMF (1 mL) and the reaction mixture was stirred for 20 h at rt. The reaction mixture was then purified by flash chromatography, using a gradient of 5–70% MeOH (2% Et_3N) in CH_2Cl_2 as eluent, to give the title compound as a white solid (30 mg, 33%). ^{1}H NMR (500 MHz, $CDCl_3$) δ 7.83–7.80 (m, 1H), 7.68–7.64 (m, 1H), 7.54–7.49 (m, 1H), 7.24–7.14 (m, 2H), 6.96 (s, 1H), 6.28–6.24 (m, 1H), 4.65–4.60 (m, 1H), 4.49–4.44 (m, 2H), 3.35 (t, J = 6.4 Hz, 2H), 2.99–2.87 (m, 5H), 2.43–2.39 (m, 2H), 2.30 (s, 6H), 1.89–1.76 (m, 6H), 1.64–1.54 (m, 1H), 1.49–1.40 (m, 2H), 1.43 (s, 9H), 1.31–1.19 (m, 2H), 1.09–0.89 (m, 4H); HRMS (ESI) *m/z* calcd for $C_{32}H_{50}N_5O_3$ $[M+H]^+$ 552.3914; found 552.3864.

4.1.18. *tert*-Butyl [(*trans*-4-{[({2-[4-(2-aminoethyl)piperidin-1-yl]quinolin-4-yl}carbonyl)amino]methyl}cyclohexyl)methyl]-carbamate (34)

Sodium azide (97 mg, 1.5 mmol) was added to a solution of the intermediate mesylate used on route to **33** (300 mg, 0.5 mmol) in

DMF (3 ml) and the reaction mixture was stirred for 20 h at rt. The reaction mixture was purified by flash chromatography, using a gradient of 50–100% EtOAc in heptane as eluent, to give the azide (197 mg, 72%). Tin(II) chloride (118 mg, 0.62 mmol), Et_3N (0.26 mL, 1.86 mmol) and thiophenol (0.26 mL, 2.5 mmol) were added to a solution of the azide (93 mg, 0.17 mmol) in THF (4 mL) and the reaction mixture was stirred for 10 min at rt. The reaction mixture was concentrated in vacuo to leave a residue, which was purified by flash chromatography, using a gradient of 0–10% MeOH/CH_2Cl_2 and then a gradient of 10–75% MeOH (2% Et_3N) in CH_2Cl_2 as eluent, to give the title compound as a solid (17 mg, 19%). ^{1}H NMR (300 MHz, $CDCl_3$) δ 8.27–8.24 (m, 1H), 8.10–8.07 (m, 1H), 7.97–7.93 (m, 1H), 7.83 (s, 1H), 7.67–7.63 (m, 2H), 7.59–7.56 (m, 1H), 4.94–4.88 (m, 2H), 3.78–3.71 (m, 3H), 3.61–3.57 (m, 1H), 3.41–3.34 (m, 4H), 3.23–3.19 (m, 2H), 2.76 (s, 1H), 2.32–2.20 (m, 6H), 2.11–1.95 (m, 1H), 1.94–1.79 (m, 2H), 1.85 (s, 9H), 1.74–1.66 (m, 3H), 1.51–1.33 (m, 4H); HRMS (ESI) *m/z* calcd for $C_{30}H_{46}N_5O_3$ $[M+H]^+$ 524.3600; found 524.3592.

4.1.19. *tert*-Butyl [(*trans*-4-{[({2-[4-(aminomethyl)piperidin-1-yl]quinolin-4-yl}carbonyl)amino]methyl}-cyclohexyl)methyl]-carbamate (35)

Prepared using essentially the same procedure as described for **26** using benzyl (piperidin-4-ylmethyl)carbamate hydrochloride together with sodium hydrogen carbonate in place of piperazine to give the intermediate piperidine. A mixture of the intermediate piperidine (0.087 g, 0.14 mmol) and 5% palladium on carbon (0.080 g, 0.038 mmol) in MeOH (10 mL) was stirred under a hydrogen atmosphere at rt for 1 h. The reaction mixture was filtered and the filtrate was concentrated in vacuo to leave a residue, which was purified by HPLC using a gradient of 10–90% mobile phase A (100% CH_3CN) over 20 min (mobile phase B = water/CH_3CN/HCO_2H 95:5:0.2) as eluent to give the title compound as a solid (34 mg, 49%). ^{1}H NMR (600 MHz, DMSO/DMSO-d_6*) δ 8.58 (t, J = 5.8 Hz, 1H), 8.32 (s, 2H), 7.76 (d, J = 8.3 Hz, 1H), 7.54 (d, J = 8.2 Hz, 1H), 7.49 (t, J = 7.6 Hz, 1H), 7.19 (t, J = 7.5 Hz, 1H), 7.15 (s, 1H), 6.76 (t, J = 5.7 Hz, 1H), 4.54 (d, J = 13.5 Hz, 2H), 3.31 (s, 5H), 3.13 (t, J = 6.1 Hz, 2H), 2.89 (t, J = 11.8 Hz, 2H), 2.74 (t, J = 6.3 Hz, 2H), 2.62–2.59 (m, 2H), 2.05–2.04 (m, J = 0.6 Hz, 2H), 1.82–1.65 (m, 6H), 1.51–1.43 (m, 1H), 1.34 (s, 9H), 1.31–1.24 (m, 1H), 1.18–1.09 (m, 2H), 0.96–0.78 (m, 4H); HRMS (ESI) *m/z* calcd for $C_{29}H_{44}N_5O_3$ $[M+H]^+$ 510.3444; found 510.3450.

4.1.20. *tert*-Butyl {[*trans*-4-({[(2-{3-[2-(dimethylamino)ethoxy]-azetidin-1-yl}-quinolin-4-yl)carbonyl]-amino}methyl)cyclo-hexyl]methyl}carbamate (36)

The first step to the intermediate 3-hydroxyazetidine was prepared by the method described in **26** using azetidin-3-ol in place of piperazine. Sodium hydride (60% in mineral oil, 21 mg, 0.53 mmol) was then added to the intermediate 3-hydroxyazetidine (0.10 g, 0.21 mmol) in DMF (2 mL) at 0 °C. After 30 min 2-chloro-*N,N*-dimethylethanamine hydrochloride (34 mg, 0.23 mmol) was added and the reaction mixture was stirred at 50 °C for 16 h. The reaction mixture was filtered and purified by HPLC, using a gradient of 30–100% CH_3CN and 0.2% NH_3 buffer as eluent to give the title compound as a solid (10 mg, 9%). ^{1}H NMR (600 MHz, $CDCl_3$) δ 7.87 (d, J = 8.6 Hz, 1H), 7.72 (d, J = 8.4 Hz, 1H), 7.58–7.53 (m, 1H), 7.26–7.23 (m, 1H), 6.61 (s, 1H), 5.97 (t, J = 5.8 Hz, 1H), 4.60–4.54 (m, 1H), 4.51–4.46 (m, 1H), 4.38–4.33 (m, 2H), 4.09 (dd, J = 9.0, 4.3 Hz, 2H), 3.54 (t, J = 5.6 Hz, 2H), 3.38 (t, J = 6.4 Hz, 2H), 2.98 (t, J = 6.0 Hz, 2H), 2.53 (t, J = 5.6 Hz, 2H), 2.27 (s, 6H), 1.89–1.79 (m, 4H), 1.61–1.52 (m, 1H), 1.45–1.38 (m, 1H), 1.43 (s, 9H), 1.09–0.93 (m, 4H); HRMS (ESI) *m/z* calcd for $C_{30}H_{46}N_5O_4$ $[M+H]^+$ 540.3550; found 540.3500.

4.1.21. *tert*-Butyl ({*trans*-4-[({[2-(4-{2-[(2-methoxyethyl)-amino]ethyl}piperidin-1-yl)quinolin-4-yl]carbonyl}amino)-methyl]cyclohexyl}methyl)carbamate (37)

Oxalyl chloride (0.26 mL, 3.1 mmol) was added dropwise to a solution of DMSO (0.44 mL, 6.2 mmol) in CH_2Cl_2 (15 mL) at −78 °C. A solution of **32** (0.54 g, 1.0 mmol) in CH_2Cl_2 (10 mL) was added in portions at −78 °C. The mixture was stirred for 30 min and then Et_3N (2 mL, 14.5 mmol) was added. The reaction mixture was warmed to rt and stirred for 30 min and then diluted with CH_2Cl_2 (100 mL) and water was added. The layers were separated and the aq layer was extracted with CH_2Cl_2 (50 mL). The combined organic layers were dried (Na_2SO_4), filtered and concentrated in vacuo to leave a residue, which was purified by HPLC using a gradient of 10–95% mobile phase A (100% CH_3CN) over 25 min (mobile phase B = 5% CH_3CN + 95% 0.1 M HCO_2H) as eluent. The required fractions were concentrated in vacuo to leave the water phase, which was diluted further with water and pH of the solution was raised to 11 by adding saturated aq sodium carbonate solution and extracted with EtOAc. The combined organic layers were dried (Na_2SO_4), filtered and concentrated in vacuo to leave the intermediate aldehyde (0.52 g, 96%). A mixture of the aldehyde (100 mg, 0.19 mmol), 3-hydroxy-azetidine hydrochloride (31 mg, 0.29 mmol), and Et_3N (0.053 mL, 0.38 mmol) in EtOH (3 mL) was stirred at rt for 5 min. Sodium triacetoxyborohydride (73 mg, 0.34 mmol) was then added and the reaction mixture was heated in a microwave reactor at 120 °C for 10 min. The reaction mixture was concentrated in vacuo to leave a residue, which was purified by HPLC, using a gradient of 30–100% CH_3CN and 0.2% NH_3 buffer as eluent to give the title compound as a white solid (71 mg, 64%). ^{1}H NMR (600 MHz, DMSO/DMSO-d_6*) δ 8.57 (t, J = 5.8 Hz, 1H), 7.76–7.74 (m, 1H), 7.54–7.51 (m, 1H), 7.50–7.46 (m, 1H), 7.19–7.16 (m, 1H), 7.11 (s, 1H), 6.76 (t, J = 5.8 Hz, 1H), 4.51–4.47 (m, 2H), 4.13–4.08 (m, 1H), 3.47–3.44 (m, 2H), 3.12 (t, J = 6.2 Hz, 2H), 2.89–2.83 (m, 2H), 2.74 (t, J = 6.3 Hz, 2H), 2.61–2.58 (m, 2H), 2.39–2.35 (m, 2H), 1.79–1.65 (m, 6H), 1.60–1.52 (m, 1H), 1.50–1.43 (m, 1H), 1.34 (s, 9H), 1.30–1.24 (m, 1H), 1.20–1.16 (m, 2H), 1.11–1.03 (m, 2H), 0.94–0.78 (m, 4H); HRMS (ESI) *m/z* calcd for $C_{33}H_{50}N_5O_4$ $[M+H]^+$ 580.3863; found 580.3870.

4.1.22. Ethyl {[*trans*-4-({[(2-{4-[2-(dimethylamino)ethyl]-piperidin-1-yl}quinolin-4-yl)carbonyl]-amino}methyl)cyclo-hexyl]-methyl}carbamate (38)

TFA (3 mL) was added to **33** (106 mg, 0.19 mmol) in CH_2Cl_2 and the reaction mixture was stirred at rt for 3 h. Toluene was added and the reaction mixture was concentrated in vacuo to leave the crude amine, which was used directly in the next step with no further purification. Ethyl chloroformate (25 mg, 0.23 mmol) was added to a solution of the crude amine and Et_3N (175 mg, 1.73 mmol) in THF at 0 °C and the reaction mixture was stirred at rt for 16 h. MeOH was added and the reaction mixture was concentrated in vacuo to leave a residue, which was purified by HPLC using a gradient of 30–100% mobile phase A (100% CH_3CN) over 30 min (mobile phase B = 5% CH_3CN + 95% 0.1 M NH_4OAc) to give the title compound as a solid (65 mg, 65% yield over 2 steps). ^{1}H NMR (600 MHz, DMSO/DMSO-d_6*) δ 8.57 (t, J = 5.7 Hz, 1H), 7.75 (d, J = 8.1 Hz, 1H), 7.53 (d, J = 8.2 Hz, 1H), 7.51–7.46 (m, 1H), 7.17 (t, J = 7.5 Hz, 1H), 7.12 (s, 1H), 7.03 (t, J = 5.7 Hz, 1H), 4.50 (d, J = 13.1 Hz, 2H), 3.93 (dd, J = 14.1, 7.1 Hz, 2H), 3.12 (t, J = 6.2 Hz, 2H), 2.87 (t, J = 11.8 Hz, 2H), 2.79 (t, J = 6.3 Hz, 2H), 2.29–2.23 (m, 2H), 2.12 (s, 6H), 1.80–1.65 (m, 6H), 1.62–1.54 (m, 1H), 1.51–1.42 (m, 1H), 1.36–1.26 (m, 3H), 1.15–1.06 (m, 5H), 0.95–0.78 (m, 4H); HRMS (ESI) *m/z* calcd for $C_{30}H_{46}N_5O_3$ $[M+H]^+$ 524.3600; found 524.3600.

4.1.23. Tetrahydro-2*H*-pyran-4-yl {[*trans*-4-({[(2-{4-[2-(di-methylamino)ethyl]piperidin-1-yl}quinolin-4-yl)carbonyl]-amino}-methyl)cyclohexyl]methyl}carbamate (39)

HCl (4 M in 1,4-dioxane, 6 mL, 24 mmol) was added to a solution of **33** (0.2 g, 0.36 mmol) in a mixture of 1,4-dioxane and water 1:1 (6 mL) and the reaction mixture was stirred at rt for 15 min. The reaction mixture was concentrated in vacuo to leave the crude amine (0.36 g, 98%) that was used with no further purification. A solution of 4-nitrophenyl tetrahydro-2*H*-pyran-4-yl carbonate (**42**, 75 mg, 0.28 mmol) in THF (3 mL) and Et_3N (0.27 mL, 1.94 mmol) was added to a solution of the amine (99 mg, 0.22 mmol) in THF (2 mL) and the reaction mixture was stirred at 40 °C for 3 h and then at rt for 16 h. The reaction mixture was concentrated in vacuo to leave a residue which was purified by flash chromatography, using a mixture of 2–25% MeOH in CH_2Cl_2 as eluent, to give the title compound as a solid (16 mg, 13%). ^{1}H NMR (600 MHz, DMSO/DMSO-d_6*) δ 8.57 (t, J = 5.8 Hz, 1H), 7.75 (d, J = 8.2 Hz, 1H), 7.54–7.51 (m, 1H), 7.50–7.46 (m, 1H), 7.19–7.15 (m, 1H), 7.12 (s, 1H), 7.08 (t, J = 5.8 Hz, 1H), 4.66–4.59 (m, 1H), 4.53–4.46 (m, 2H), 3.80–3.72 (m, 2H), 3.40–3.33 (m, 2H), 3.12 (t, J = 6.2 Hz, 2H), 2.90–2.83 (m, 2H), 2.80 (t, J = 6.3 Hz, 2H), 2.26–2.19 (m, 2H), 2.09 (s, 6H), 1.82–1.64 (m, 8H), 1.62–1.53 (m, 1H), 1.52–1.39 (m, 3H), 1.37–1.26 (m, 3H), 1.16–1.05 (m, 2H), 0.95–0.78 (m, 4H); HRMS (ESI) m/z calcd for $C_{33}H_{50}N_5O_4$ $[M+H]^+$ 580.3863; found 580.3875.

4.1.24. 2,2-Dimethylpropyl {[*trans*-4-({[(2-{4-[2-(dimethylamino)ethyl]piperidin-1-yl}quinolin-4-yl)-carbonyl]amino}-methyl)cyclohexyl]methyl}carbamate (40)

2,2-Dimethylpropyl chlorocarbonate (32 μL, 0.21 mmol) was added to a solution of the intermediate amine, from on route to **39** (100 mg, 0.18 mmol), and DIPEA (0.31 mL, 1.8 mmol) in CH_2Cl_2 (5 mL) and the reaction mixture was stirred at rt for 10 min. The reaction mixture was concentrated in vacuo to leave a residue, which was purified by HPLC using a gradient of 10–90% mobile phase A (100% CH_3CN) over 20 min (mobile phase B = water/CH_3CN/HCO_2H 95:5:0.2) as eluent to give the title compound as a white solid (75 mg, 74%). ^{1}H NMR (500 MHz, $CDCl_3$) δ 7.88–7.80 (m, 1H), 7.71–7.64 (m, 1H), 7.57–7.49 (m, 1H), 7.28–7.19 (m, 1H), 7.01 (s, 1H), 6.20–6.12 (m, 1H), 4.80–4.70 (m, 1H), 4.55–4.46 (m, 2H), 3.79–3.70 (m, 2H), 3.42–3.33 (m, 2H), 3.08–2.99 (m, 2H), 2.98–2.86 (m, 2H), 2.72–2.62 (m, 2H), 2.48 (s, 6H), 1.93–1.75 (m, 6H), 1.68–1.53 (m, 4H), 1.50–1.39 (m, 1H), 1.34–1.21 (m, 2H), 1.11–0.88 (m, 4H), 0.92 (s, 9H); HRMS (ESI) m/z calcd for $C_{33}H_{52}N_5O_3$ $[M+H]^+$ 566.4070; found 566.4029.

4.1.25. [*trans*-4-({[(2-{4-[2-(Dimethylamino)ethyl]piperidin-1-yl}quinolin-4-yl)carbonyl]amino}methyl)-cyclohexyl]methyl *tert*-butylcarbamate (41)

A 0.5 M aqueous solution of lithium hydroxide (0.639 mL, 0.32 mmol) was added to a solution of methyl *trans*-4-({[(2-{4-[2-(dimethylamino)ethyl]piperidin-1-yl-}quinolin-4-yl)carbonyl]-amino}methyl)cyclohexanecarboxylate **44**[16] (0.13 g, 0.27 mmol) in THF (6 mL). The reaction mixture was stirred at rt for 16 h. Additional 0.5 M aqueous solution of lithium hydroxide (0.639 mL, 0.32 mmol) was added and the reaction mixture was stirred at rt for 16 h. Toluene was added and the reaction mixture was concentrated in vacuo to give the crude carboxylic acid that was used with no further purification. 4-Methylmorpholine (0.030 mL, 0.27 mmol) and butyl carbonochloridate (0.034 mL, 0.27 mmol) were added to the acid (0.27 mmol) in THF (10 mL) and the reaction mixture was stirred for 30 min. Sodium borohydride (0.014 g, 0.38 mmol) followed by MeOH (20 mL) were added and the reaction mixture was stirred at rt for 16 h. The reaction mixture was then partitioned between CH_2Cl_2 and saturated aqueous NaCl. The aqueous phase was extracted with CH_2Cl_2 and the combined organic phases were dried (phase separator) and concentrated in vacuo to leave a residue which was purified by preparative HPLC (20→95% CH_3CN in 0.2% aqueous NH_3 as eluent) to give 2-{4-[2-(dimethylamino)ethyl]piperidin-1-yl}-*N*-{[*trans*-4-(hydroxyl-methyl)cyclohexyl]methyl}-quinoline-4-carboxamide (0.017 g, 14%). 2-Isocyanato-2-methylpropane (0.017 mL, 0.15 mmol) was added to the carboxamide (0.017 g, 0.04 mmol) in pyridine (0.5 mL) and the reaction mixture was stirred at 70 °C for 16 h. Additional 2-isocyanato-2-methylpropane (0.1 mL, 0.9 mmol) was added and the reaction mixture was stirred at 70 °C for 32 h and then concentrated in vacuo and the residue was purified by reversed phase HPLC, using a gradient of 30→100% CH_3CN and 0.2% NH_3 buffer as eluent to give the title compound as a solid (6.5 mg, 31%). ^{1}H NMR (600 MHz, DMSO/DMSO-d_6*) δ 8.64 (t, J = 5.8 Hz, 1H), 7.82–7.76 (m, 1H), 7.57 (d, J = 7.6 Hz, 1H), 7.55–7.51 (m, 1H), 7.24–7.20 (m, 1H), 7.17 (s, 1H), 4.55 (d, J = 13.1 Hz, 2H), 3.77–3.67 (m, 2H), 3.17 (t, J = 6.3 Hz, 2H), 2.96–2.87 (m, 2H), 2.55 (s, 1H), 2.38–2.31 (m, 2H), 2.27–2.14 (m, 6H), 1.90–1.72 (m, 6H), 1.68–1.58 (m, 1H), 1.57–1.47 (m, 2H), 1.43–1.35 (m, 2H), 1.21 (s, 9H), 1.19–1.09 (m, 2H), 1.03–0.92 (m, 4H); HRMS (ESI) m/z calcd for $C_{32}H_{50}N_5O_3$ $[M+H]^+$ 552.3914; found 552.3942.

4.2. hACC2 and hACC1 in vitro assay description

Human recombinant ACC1 and ACC2 were assayed by determining the amount of inorganic phosphate (P_i) generated. Pre-incubation of 15 μL enzyme together with 0.75 μL DMSO ± compound for 5 min was done before the reaction was initiated by the addition of 10 μL substrate. The reaction was carried out in 384-well plates at 37 °C containing the following constituents (n = 2); 1 mM ATP, 0.4 mM acetyl-CoA, 20 mM citrate, 50 mM Hepes (pH 7.5), 12.5 mM $NaHCO_3$, 20 mM $MgAc_2 \times 4H_2O$, 1.5 mM $MgSO_4 \times 7H_2O$, 1 mM TCEP, 0.025% BSA, compound at different concentrations, ACC1 and ACC2 diluted to generate signals resulting in assay Z' >0.5. After 1.5 h the reaction was stopped by addition of 74 μL of water followed by extensive mixing, split and transfer of 2 × 40 μL to a read-plate encompassing 30 μL H_2O per well (n = 2→n = 4). Colour reaction was initiated by addition of 30 μL malachite green reagent per well and allowed 15 min before absorbance reading of the plates at 660 nm. The malachite green reagent was prepared by mixing 16.4 mL ammonium molybdate solution (7.5%), 1.64 mL Tween (11%) with 82 mL Malachite Green/H_2SO_4-solution (0.7 g Malachite Green to 1000 mL of 10% (v/v) H_2SO_4). All compounds were tested in triplicate at 10 different concentrations. Control compound (0%, 50% and 100% effect) was included on each plate. The inhibitory effect of a compound was calculated by %inhibition = 100 × [(X − Max)/(Min − Max)], where X is the readout value in the compound well. Min is the average signal for 100% inhibition and Max is the average signal for 0% inhibition in the control wells. Curve fitting was done using the following equation: y = (A + ((B − A)/(1 + ((x/C)^D)))) where A and B represents the curve bottom (% inhibition) and the total amplitude (% inhibition), respectively, whereas C and D are the apparent IC_{50} and curve slope, respectively. Some compounds were tested using a slightly modified protocol at rt instead of 37 °C. The data transferred well between assays and no temperature effect was observed with these compounds. See Supplementary data for full protocol.

4.3. X-ray structure determination

Hexa-histidine tagged ACC2 CT-domain (aa1685–2431) from bovine was over-expressed in *Escherichia coli* BL21 gold (DE3) cells and purified using Ni^{2+}-NTA affinity chromatography. The histidine-tag was removed by thrombin and separated by another Ni^{2+}-NTA affinity chromatography step followed by size exclusion chromatography in a buffer containing 20 mM Tris, 200 mM NaCl,

5% glycerol and 1 mM TCEP at pH 7. The protein was concentrated to around 20 mg/mL before crystallization at 20 °C using the hanging-drop method. The precipitating solution consisted of 20–25% PEG4000, 400–800 mM LiCl, 100 mM Tris pH 8–8.5. The ligand complex was prepared by soaking crystals in 15 mM **28** for 3 days before freezing the crystals in liquid nitrogen using 20% glycerol in mother liquor solution as cryo-protectant. X-ray data was collected at 100 K on beam-line ID29 at the ESRF. The structure was solved with the molecular replacement using the yeast ACC2 (PDB entry 1OD2) as search model. The final resolution was 2.4 Å, with $R = 23.1$, $R_{free} = 28.3$. The structure has been deposited in the PDB where further refinement details can be found (2X24).

4.4. Inhibition of ACCs in vivo

Experimental procedures were in accordance with Swedish laws governing the use of animals for experimental purposes and were approved by the Local Ethics Review on Animal Experiments in Gothenburg region. In vivo inhibition of ACCs was assessed indirectly based on the extent of substance induced malonyl-CoA lowering in the liver of male obese Zucker rats. On the day of the experiment male obese Zucker rats, weighing 370–540 g, were individually housed in a clean cage without food but with access to water at 07:00. The animals were weighed and anesthetized with an intraperitoneal injection of Na-thiobutabarbital (Inactin®; RBI, Natick, MA), 180 mg/kg BW at 10:00. They were tracheotomized with PE 240 tubing and breathed spontaneously. One catheter (PE 50 tubing) was placed in a carotid artery for blood sampling. Two catheters (PE 50) were placed in one jugular vein for substance/vehicle infusion and thiobutabarbitol top-up dosing, respectively. The arterial catheter was maintained patent throughout the experiment by continuous infusion (10 μL/min) of a sterile saline solution containing sodium citrate (20.6 mM). The acute experimental phase commenced 13:00 following a 1.5 h post-surgery stabilization period. Body temperature was monitored using a rectal thermocouple and maintained at 37.5 °C by means of external heating. Substances were administered as constant intravenous infusions for 2 h. At the end of this period, substance infusion was stopped and the deeply anaesthetized rat was moved to the dissection table where the liver tissue for malonyl-CoA content was excised and frozen in liquid N_2 as quickly as possible. Blood was then quickly collected from the carotid cannula for substance analysis in plasma. The frozen liver samples, immersed in liquid N_2 were broken into smaller pieces (50–100 mg) and weighed into 2 mL Micro tubes (PP, Sarstedt, Numbrecht, Germany) and stored in a −80 °C freezer awaiting malonyl-CoA. Blood for substance analysis was collected into 500 μL Microvette® 500 K3E tubes (Sarstedt), plasma separated by centrifugation (10,000 g, 1 min, 4 °C) and plasma stored at −20 °C awaiting analysis.

4.5. Analysis of malonyl-CoA in tissue by ion-pair-HPLC-tandem-mass spectrometry

Malonyl-CoA was analysed in small tissue samples by a cold, semi-automated homogenization and extraction method followed by separation by ion-pair HPLC and detection by negative electrospray tandem mass spectrometry. The method is based on cryogenic sampling of 50–100 mg tissue in 2 mL Sarstedt polypropylene screw cap micro tubes (Sarstedt, product 72.694.007) prefilled with six yttrium stabilized (3 mm) zirconium oxide beads (Retsch, product 05.368.0090). Simultaneous and automated batch homogenization and initial extraction with the Precellys-24 (Bertin, France) was performed for 2 × 15 s at power 5000 after addition of 0.5 mL –20 °C cold extraction buffer (40% MeOH, 5% TFA and 0.01% dithioerythritol (DTE)), 50 μL internal standard (15 μM $^{13}C_3$–malonyl-CoA) and 100 μL 30% bovine serum albumin in phosphate buffered saline (Sigma, product A9576–50 mL). Complete extraction and sample purification (removal of lipids) at −20 °C with the Mixer Mill 300 (Retsch, Germany) was performed for 5 min at 25 Hz after addition of 0.5 mL $CHCl_3$. The upper aqueous sample extract was evaporated to dryness in HPLC glass vials at 50 °C under a stream of nitrogen, after centrifugation of samples at 3000 G for 10 min, and analytes were dissolved in 100 μL injection solvent (0.5% TFA and 2% CH_3CN). Separation was achieved in only 8 min using a binary solvent system and a gradient run (0% B from 0.0–0.2 min then 100% B from 3.5–5.5 min and 0% B from 5.6 to 7.6 min) where phase A was 10 mM NH_4OAc, 5 mM AcOH, 10 mM DIPEA and 2% CH_3CN and phase B was 25% phase A in CH_3CN. The column was a Hypersil Gold C18, 30 × 2.1 mm, 1.9 μm (Thermo, product 25002–032130) connected to a precolumn (Thermo, product 25,003–012101) and a 0.5 μm filter. Malonyl-CoA and the internal standard were then determined quantitatively by negative electrospray tandem-MS using an Ultima PT mass spectrometer (Micromass, England) The electrospray probe was operated at 120 °C, with the capillary at 2.8 kV, desolvation gas at 350 °C, cone gas flow at 50 L/hour and the desolvation gas flow at 800 L/hour. The waste valve solvent delay was on from 0–2 min and 4–5 min. The mass spectrometer was operated in multiple reactions monitoring mode with a cone voltage of 50 kV and dwell time of 0.050 s for all analytes. The mass transitions were 852 > 808 (malonyl-CoA), 855 > 810 ($^{13}C_3$–malonyl-CoA), and optionally 808 > 408 for acetyl-CoA. The collision energy was 25 eV (malonyl-CoA and $^{13}C_3$–malonyl-CoA) or 35 eV (acetyl-CoA). For quantitative analysis, tissue samples were calibrated against 5-point calibration curves ranging from 160 nM to 100 μM prepared in extraction buffer diluted 10 times with 40% methanol and stored at −80 °C. Calibration samples were processed as tissue samples. The detection limits were less than 1 pmol on-column.

4.6. Substance exposures

Normalized substance exposures were calculated as, Exposure = Cp_{free}/IC_{50}, where IC_{50} is the estimated free in vitro concentration required to half maximally inhibit rat ACC2 and Cp_{free} is the estimated free plasma concentration obtained from the measured compound concentration Cp as $Cp_{free} = f_u \times Cp$, where f_u is the unbound fraction of substance in plasma measured in separate experiments under standard conditions (see Supplementary data for measurement of plasma protein binding).

Acknowledgments

We thank Lisa Alderin, Åsa Einarsson, Henrik Gradén and Åsa Månsson for synthesis of some compounds and all involved in purification and analysis and Anna-Karin Asztély, Anita Dellsén, Pia Hansson, Pia Thalén, Ann Kjellstedt, Zulma Santisteban and Helena von Bahr for help with in vitro and in vivo experiments. We also thank Sara Moses, Sven Sjögren and Carl-Gustav Sigfridsson, Johan Wernevik and Christer Westerlund for helpful discussions.

Supplementary data

Supplementary data (experimental details for the synthesis of intermediates on route to **18**, **21**, **29** and **41** as well as **42** and **44**. Further details on the enzyme assay, details of enzyme preparation and activity measurement and procedures for plasma protein binding, solubility, stability in HLM and caco-2 permeability measurements. Explanation of torsional scan analysis, sequence

alignments for hACC1, hACC2, rat ACC2 and bACC2, test substance concentrations in terminal plasma samples and substance partitioning in plasma: bound versus free fractions) associated with this article can be found, in the online version, at doi:10.1016/j.bmc.2011.04.014.

References and notes

1. Data was obtained from the World Health Organization website: http://www.who.int/diabetes/en/.
2. Corbett, J. W. *Expert Opin.* **2009**, *19*, 943.
3. Polakis, S. E.; Guchhait, R. B.; Zwergel, E. S.; Lane, M. D.; Cooper, T. G. *J. Biol. Chem.* **1974**, *249*, 6657.
4. Harwood, H. J., Jr.; Petras, S. F.; Shelly, L. D.; Zaccaro, L. M.; Perry, D. A.; Makowski, M. R.; Hargrove, D. M.; Martin, K. A.; Tracey, W. R.; Chapman, J. G.; Magee, W. P.; Dalvie, D. K.; Soliman, V. F.; Martin, W. H.; Mularski, C. J.; Eisenbeis, S. A. *J. Biol. Chem.* **2003**, *278*, 37099.
5. (a) Harwood, H. J., Jr. *Expert Opin. Ther. Targets* **2005**, *9*, 267; (b) Tong, L.; Harwood, H. J., Jr. *J. Cell. Biochem.* **2006**, *99*, 1476.
6. An, J.; Muoio, D. M.; Shiota, M.; Fujimoto, Y.; Cline, G. W.; Shulman, G. I.; Koves, T. R.; Stevens, R.; Millington, D.; Newgardet, C. B. *Nat. Med.* **2004**, *10*, 268.
7. (a) Abu-Elheiga, L.; Matzuk, M. M.; Abo-Hashema, K. A. H.; Wakil, S. J. *Science* **2001**, *291*, 2613; (b) Abu-Elheiga, L.; Oh, W.; Kordari, P.; Wakil, S. J. *Proc. Natl. Acad. Sci. U.S.A.* **2003**, *100*, 10207; (c) Oh, W.; Abu-Elheiga, L.; Kordari, P.; Gu, Z.; Shaikenov, T.; Chirala, S. S.; Wakil, S. J. *Proc. Natl. Acad. Sci. U.S.A.* **2005**, *102*, 1384.
8. Savage, D. B.; Choi, C. S.; Samuel, V. T.; Lui, Z. X.; Zhang, D.; Wang, A.; Zhang, X. M.; Cline, G. W.; Yu, X. X.; Geisler, J. G.; Bhanot, S.; Monia, B. M.; Shulman, G. I. *J. Clin. Invest.* **2006**, *116*, 817.
9. Abu-Elheiga, L.; Matzuk, M. M.; Kordari, P.; Oh, W.; Shaikenov, T.; Gu, Z.; Wakil, S. J. *Proc. Natl. Acad. Sci. U.S.A.* **2005**, *102*, 12011.
10. Olson, D. P.; Pulinilkunnil, T.; Cline, G. W.; Shulman, G. I.; Lowell, B. B. *Proc. Natl. Acad. Sci. U.S.A.* **2010**, *107*, 7598.
11. (a) Corbett, J. W.; Harwood, H. J., Jr. *Recent Patents Cardiovasc. Drug Disc.* **2007**, *2*, 162; (b) Clark, R. F.; Zhang, T.; Wang, X.; Wang, R.; Zhang, X.; Camp, H. S.; Beutel, B. A.; Sham, H. L.; Gu, Y. G. *Bioorg. Med. Chem. Lett.* **2007**, *17*, 1961; (c) Shinde, P.; Srivastava, S. K.; Odedara, R.; Tuli, D.; Munshi, S.; Patel, J.; Zambad, S. P.; Sonawane, R.; Gupta, R. C.; Chauthaiwale, V.; Dutt, C. *Bioorg. Med. Chem. Lett.* **2009**, *19*, 949; (d) Haque, T. S.; Liang, N.; Golla, R.; Seethala, R.; Ma, Z.; Ewing, W. R.; Cooper, C. B.; Pelleymounter, M.-A.; Poss, M. A.; Cheng, D. *Bioorg. Med. Chem. Lett.* **2009**, *19*, 5872; (e) Corbett, J. W.; Freeman-Cook, K. D.; Elliott, R.; Vajdos, F.; Rajamohan, F.; Kohls, D.; Marr, E.; Zhang, H.; Tong, L.; Tu, M.; Murdande, S.; Doran, S. D.; Houser, J. A.; Song, W.; Jones, C. J.; Coffey, S. B.; Buzon, L.; Minich, M. L.; Dirico, K. J.; Tapley, S.; McPherson, R. K.; Sugarman, E.; Harwood, H. J., Jr.; Esler, W. *Bioorg. Med. Chem. Lett.* **2010**, *20*, 2383; (f) Chonan, T.; Tanaka, H.; Yamamoto, D.; Yashiro, M.; Oi, T.; Wakasugi, D.; Ohoka-Sugita, A.; Io, F.; Koretsune, H.; Hiratate, A. *Bioorg. Med. Chem. Lett.* **2010**, *20*, 3965.
12. Shen, Y.; Volrath, S. L.; Weatherley, S. C.; Elich, T. D.; Anderson, R.; Tong, L. Patent WO06017515, 2006.
13. Anderson, G. W.; McGregor, A. C. *J. Am. Chem. Soc.* **1957**, *79*, 6180.
14. Risaliti, A. *Ric. Scient.* **1958**, *28*, 561.
15. Minakata, S.; Komatsu, M.; Ohshiro, Y. *Synthesis* **1992**, 661.
16. See Supplementary data for synthesis description.
17. Log *D* measurement based on chromatographic retention times (log *k*') from a method similar to that described in Valkó, K.; Bevan, C.; Reynolds, D. *Anal. Chem.* **1997**, *69*, 2022.
18. Yee, S. *Pharm. Res.* **1997**, *14*, 763.
19. Chiou, W. L.; Robbiel, G.; Chung, S. M.; Wu, T.-C.; Ma, C. *Pharm. Res.* **1998**, *15*, 1474.
20. (a) Gleeson, M. P. *J. Med. Chem.* **2008**, *51*, 817; (b) Waring, M. J. *Expert Opin. Drug Disc.* **2010**, *5*, 235.
21. (a) Leeson, P. D.; Springthorpe, B. *Nat. Rev. Drug Disc.* **2007**, *6*, 881; (b) Ryckmans, T.; Edwards, M. P.; Horne, V. A.; Correia, A. M.; Owen, D. R.; Thompson, L. R.; Tran, I.; Tutt, M. F.; Young, T. *Bioorg. Med. Chem. Lett.* **2009**, *19*, 4406.
22. Zhang, H.; Tweel, B.; Li, J.; Tong, L. *Structure* **2004**, *12*, 1683.
23. Madauss, K. P.; Burkhart, W. A.; Consler, T. G.; Cowan, D. J.; Gottschalk, W. K.; Miller, A. B.; Short, S. A.; Tran, T. B.; Williams, S. P. *Acta Crystallogr., Sect. D* **2009**, *65*, 449.
24. Waring, M. J. *Bioorg. Med. Chem. Lett.* **2009**, *19*, 2844.
25. Sequence Alignments for hACC1, hACC2, rat ACC2 and bACC2 are shown in Supplementary data.
26. (a) Becke, A. D. *J. Chem. Phys.* **1993**, *98*, 5648; (b) Lee, C.; Yang, W.; Parr, R. G. *Phys. Rev. B* **1988**, *37*, 785; (c) Stephens, P. J.; Devlin, F. J.; Chabalowski, C. F.; Frisch, M. J. *J. Phys. Chem.* **1994**, *98*, 11623.
27. Abu-Elheiga, L.; Almarza-Ortega, D. B.; Baldini, A.; Wakil, S. J. *J. Biol. Chem.* **1997**, *272*, 10669.
28. Redfern, W.; Carlsson, L.; Davis, A. S.; Lynch, W. G.; MacKenzie, I.; Palethorpe, S.; Siegl, P. K. S.; Strang, I.; Sullivan, A. T.; Wallis, R.; Camm, A. J.; Hammond, T. G. *Cardiovasc. Res.* **2003**, *58*, 32.
29. Rat ACC2 and ACC1 in vitro assay used to test compounds **1**, **33** and **37** was performed in an analogous manner to the hACC2 and hACC1 in vitro assays described in the Section 4 using rat ACC2 and ACC1 in place of hACC2 and hACC1, respectively.